

Contents lists available at ScienceDirect

# **Automatica**

journal homepage: www.elsevier.com/locate/automatica



# Backstepping control of continua of linear hyperbolic PDEs and application to stabilization of large-scale n+m coupled hyperbolic PDE systems\*



Jukka-Pekka Humaloja\*, Nikolaos Bekiaris-Liberis

Department of Electrical and Computer Engineering, Technical University of Crete, University Campus, Akrotiri, Chania, 73100, Greece

#### ARTICLE INFO

Article history: Received 30 October 2024 Received in revised form 24 July 2025 Accepted 2 September 2025

Keywords:
Backstepping control
Hyperbolic PDEs
Large-scale systems
PDE continua

#### ABSTRACT

We develop a backstepping control design for a class of continuum systems of linear hyperbolic PDEs, described by a coupled system of an ensemble of rightward transporting PDEs and a (finite) system of m leftward transporting PDEs. The key analysis challenge of the design is to establish well-posedness of the resulting ensemble of kernel equations, since they evolve on a prismatic (3-D) domain and inherit the potential discontinuities of the kernels for the case of n+m hyperbolic systems. We resolve this challenge generalizing the well-posedness analysis of Hu, Di Meglio, Vazquez, and Krstic to continua of general, heterodirectional hyperbolic PDE systems, while also constructing a proper Lyapunov functional.

Since the motivation for addressing such PDE systems continua comes from the objective to develop computationally tractable control designs for large-scale PDE systems, we then introduce a methodology for stabilization of general n+m hyperbolic systems, constructing stabilizing backstepping control kernels based on the continuum kernels derived from the continuum system counterpart. This control design procedure is enabled by establishing that, as n grows, the continuum backstepping control kernels can approximate (in certain sense) the exact kernels, and thus, they remain stabilizing (as formally proven). This approach guarantees that complexity of computation of stabilizing kernels does not grow with the number n of PDE systems components. We further establish that the solutions to the n+m PDE system converge, as  $n\to\infty$ , to the solutions of the corresponding continuum PDE system.

We also provide a numerical example in which the continuum kernels can be obtained in closed form (in contrast to the large-scale kernels), thus resulting in minimum complexity of control kernels computation, which illustrates the potential computational benefits of our approach.

© 2025 The Author(s). Published by Elsevier Ltd. This is an open access article under the CC BY license (http://creativecommons.org/licenses/by/4.0/).

## 1. Introduction

#### 1.1. Motivation

Stabilization of large-scale systems of general, n+m heterodirectional linear hyperbolic PDEs can be achieved via back-stepping, see, for example, Anfinsen and Aamo (2019), Auriol and Bresch-Pietri (2022), Auriol and Di Meglio (2016), Coron, Hu, and Olive (2017), Di Meglio, Bribiesca Argomedo, Hu, and

E-mail addresses: jhumaloja@tuc.gr (J.-P. Humaloja), nlimperis@tuc.gr, bekiaris-liberis@ece.tuc.gr (N. Bekiaris-Liberis).

Krstic (2018), Hu, Di Meglio, Vazquez, and Krstic (2016), Hu, Vazguez, Di Meglio, and Krstic (2019) and Ramirez, Zwart, and Gorrec (2013). Such large-scale systems of hyperbolic PDEs may be utilized to describe the dynamics of various systems with practical importance. In particular, they can be utilized to describe, traffic flow dynamics in large traffic networks (Friedrich, Göttlich, & Osztfalk, 2022; Göttlich, Herty, Moutari, & Weissen, 2021; Tumash, Canudas-de Wit, & Delle Monache, 2022; Zhang, Luan, Lu, & Prieur, 2022), as well as in multi-lane (Herty & Klar, 2003; Yu & Krstic, 2021) or multi-class traffic (Burkhardt, Yu, & Krstic, 2021; Mohan & Ramadurai, 2017); blood flow dynamics in cardiovascular networks consisting of interconnected arterial segments (Bikia, 2021; Reymond, Merenda, Perren, Rufenacht, & Stergiopulos, 2009); epidemics spreading dynamics in various geographical regions and among different age groups (Bastin & Coron, 2016; Guan et al., 2020; Iannelli, 1995; Kitsos, Besancon, & Prieur, 2022); dynamics of multi-phase flows in oil drilling

The material in this paper was partially presented at the 23rd European Control Conference in Thessaloniki, Greece on 24–27 June 2025, involving a preliminary version of Sections 2 and 3. This paper was recommended for publication in revised form by Associate Editor Miroslav Krstic under the direction of Editor Rafael Vazquez.

<sup>\*</sup> Corresponding author.

applications (Di Meglio, Kaasa, Petit, & Alstad, 2011); and water networks dynamics (Bastin & Coron, 2016; Diagne, Diagne, Tang, & Krstic, 2017). Complexity of computation of stabilizing backstepping kernels may, in general, grow with the number of PDE systems components (Humaloja & Bekiaris-Liberis, 2025a, 2025b), which may, in fact, be alleviated constructing backstepping feedback laws based on continua PDE systems counterparts (Humaloja & Bekiaris-Liberis, 2025a, 2025b). Consequently, motivated by this and the practical significance of considering largescale systems of hyperbolic PDEs, we address the problem of design of computationally tractable backstepping feedback laws for large-scale systems of n + m heterodirectional linear hyperbolic PDEs, via introduction of a control design procedure that relies on development of backstepping control laws for continua PDE systems counterparts. In fact, we note that the considered continua of PDE systems may appear in applications as such. This is the case, for example, in multi-class traffic flow models, when the vehicle classes are characterized by a continuous variable depending on driving characteristics, such as, e.g., drivers' age (see also Alleaume and Krstic (2025, Sect. I), and Yu and Krstic (2022, Ch. 9)).

#### 1.2. Literature

The first result on backstepping stabilization of a class of continua of hyperbolic PDE systems was developed in Alleaume and Krstic (2025), while a formal connection between the class of systems considered in Alleaume and Krstic (2025) and the class of n + 1 linear hyperbolic systems (Di Meglio, Vazquez, & Krstic, 2013) (for large n), as well as the application of the control design originally developed for the continuum system to the large-scale counterpart, were made in Humaloja and Bekiaris-Liberis (2025b). Therefore, besides Alleaume and Krstic (2025) and Humaloja and Bekiaris-Liberis (2025b), the present paper is related to the results on backstepping stabilization of n+m linear hyperbolic systems, see, for example, Anfinsen and Aamo (2019), Auriol and Di Meglio (2016), Coron et al. (2017), Di Meglio et al. (2018) and Hu et al. (2016, 2019), as well as to results in which PDE ensembles may arise as result of employment of Fourier transform, see, for example, Vazquez and Krstic (2008) (that deals with parabolic PDEs). In addition, as the actual motivation for our developments is to address computational complexity of backstepping designs for large-scale hyperbolic systems, papers related to computation of backstepping kernels are also relevant, in particular, Bhan, Shi, and Krstic (2024) that introduces a neural operators-based computation method, Auriol, Morris, and Di Meglio (2019) that presents a late-lumping-based approach, and Vazquez, Chen, Qiao, and Krstic (2023) that relies on power series representations of the kernels (even though these results do not explicitly aim at addressing computational complexity with respect to increasing number of systems components). Here we address the previously unattempted problems of backstepping control design for the continuum counterpart of a large-scale system of n + m hyperbolic PDEs and its application for the stabilization of the original large-scale system.

# 1.3. Contributions

We start considering a continuum PDE system that may correspond to the n+m hyperbolic system as  $n\to\infty$  for which we employ the continuum PDE backstepping method. This gives rise to a continuum plus m kernel equations that are defined on a prismatic (3-D) domain that arises by continuating the triangular (2-D) domain of definition of the respective n+m kernel equations. We establish well-posedness of the kernel equations treating them on each 3-D subdomain that is spanned along the

direction of the ensemble variable from subdomains of the 2-D triangular space on which the kernels do not feature discontinuities. This allows us to then show continuity of the respective characteristic projections and to employ the successive approximations approach on each 3-D subdomain, thus generalizing the well-posedness results from Alleaume and Krstic (2025) and Hu et al. (2016, 2019) for the n + m and  $\infty + 1$  cases, respectively, to the case of a continuum plus m ( $\infty + m$ ) kernels. Such a generalization is highly nontrivial and requires a delicate technical treatment as it inherits the technical intricacies of both going from n + 1 to n + m systems, in particular, the fact that the kernels may feature discontinuities, and going from a system with finite components to a continuum, in particular, having to deal with PDEs defined on 2-D domains instead of vector-valued 1-D PDEs. We establish exponential stability (in  $L^2$ ) of the closed-loop system, constructing a Lyapunov functional.

We then consider the large-scale n + m system counterpart for which we design a feedback law employing the continuum kernels (evaluated at n points for each control input), based on the continuum approximation idea from Humaloja and Bekiaris-Liberis (2025b). We establish that the closed-loop system is exponentially stable (in  $L^2$ ) by showing that, for sufficiently large n, the exact backstepping kernels can be approximated to any desired accuracy by the continuum kernels. The proof relies on construction of a sequence of backstepping kernels that is defined such that each kernel in the sequence matches the exact kernel (in a piecewise manner with respect to the ensemble variable), while then showing that this sequence converges to the continuum kernel. This in turn implies that the approximation error of the exact control kernels can be made arbitrarily small for sufficiently large n. This gives rise to a closed-loop system that is affected by a bounded vanishing perturbation with a bound that can be made arbitrarily small, and thus, the closed-loop system remains exponentially stable, which we show constructing a Lyapunov functional. We further provide a convergence result establishing the exact convergence properties of the actual solutions of the n+m PDE system to the solutions of the continuum counterpart, which is analogous to the m = 1 case considered in Humaloja and Bekiaris-Liberis (2025b). We provide a numerical example of an n+m system for which the exact control kernels do not exhibit a closed-form solution, but the continuum kernels of the respective  $\infty + m$  system do, illustrating the computational complexity benefits of employing the continuum kernels for stabilization of the large-scale system.

## 1.4. Organization

The paper is organized as follows. In Section 2, we present a backstepping control law for  $\infty+m$  hyperbolic systems and show exponential stability of the closed-loop system. In Section 3, we show that the backstepping kernels employed in the control law are well-posed. In Section 4, we show that the  $\infty+m$  kernels can be used in constructing exponentially stabilizing control laws for large-scale n+m hyperbolic systems. In Section 5, we formally show the convergence of the solution of the n+m PDE system to the solution of the  $\infty+m$  PDE system. In Section 6, we validate the theoretical developments on a numerical example, illustrating in simulation that stabilization of the n+m system can be achieved employing the continuum kernels-based controller. In Section 7, we provide concluding remarks and discuss open problems.

#### 1.5. Notation

We use the standard notation  $L^2(\Omega;\mathbb{R})$  for real-valued Lebesgue integrable functions on a domain  $\Omega\subset\mathbb{R}^d$  for some  $d\geq 1$ . For conciseness, we occasionally use shorthand  $L^2$  for  $L^2([0,1];\mathbb{R})$ . The notations  $L^\infty(\Omega;\mathbb{R})$ ,  $C(\Omega;\mathbb{R})$ , and  $C^1(\Omega;\mathbb{R})$  denote essentially bounded, continuous, and continuously differentiable functions, respectively, on  $\Omega$ . Moreover, the notation  $f\in L^2_{\mathrm{loc}}([0,+\infty);\mathbb{R})$  means that  $f\in L^2([0,a];\mathbb{R})$  for any  $a\in\mathbb{N}$ . We denote vectors and matrices by bold symbols, and  $\|\cdot\|_\infty,\|\cdot\|_1$  denote the maximum absolute row and column sums, respectively, of a matrix (or a vector). For any  $n,m\in\mathbb{N}$ , we denote by E the space  $L^2([0,1];\mathbb{R}^{n+m})$  equipped with the inner product

$$\left\langle \left( \begin{array}{c} \mathbf{u}_1 \\ \mathbf{v}_1 \end{array} \right), \left( \begin{array}{c} \mathbf{u}_2 \\ \mathbf{v}_2 \end{array} \right) \right\rangle_E =$$

$$\int_0^1 \left( \frac{1}{n} \sum_{i=1}^n u_1^i(x) u_2^i(x) + \sum_{j=1}^m v_1^j(x) v_2^j(x) \right) dx, \tag{1}$$

which induces the norm  $\|\cdot\|_E = \sqrt{\langle \cdot, \cdot \rangle_E}$ . We also define the continuum version of E as  $n \to \infty$  by  $E_c = L^2([0, 1]; L^2([0, 1]; \mathbb{R})) \times L^2([0, 1]; \mathbb{R}^m)$ , (i.e.,  $\mathbb{R}^n$  becomes  $L^2([0, 1]; \mathbb{R})$  as  $n \to \infty$ ) equipped with the inner product

$$\left\langle \begin{pmatrix} u_1 \\ \mathbf{v}_1 \end{pmatrix}, \begin{pmatrix} u_2 \\ \mathbf{v}_2 \end{pmatrix} \right\rangle_{E_c} = \int_0^1 \left( \int_0^1 u_1(x, y) u_2(x, y) dy + \sum_{j=1}^m v_1^j(x) v_2^j(x) \right) dx, \tag{2}$$

which coincides with  $L^2([0, 1]^2; \mathbb{R}) \times L^2([0, 1]; \mathbb{R}^m)$ . Moreover, we say that a system is exponentially stable on E (resp. on  $E_c$ ) if, for any initial condition  $z_0 \in E$  (resp.  $z_0 \in E_c$ ), the (weak) solution  $z \in C([0, \infty); E)$  (resp.  $z \in C([0, \infty); E_c)$ ) of the system satisfies  $\|z(t)\|_E \leq Me^{-ct}\|z_0\|_E$  (resp.  $\|z(t)\|_{E_c} \leq Me^{-ct}\|z_0\|_{E_c}$ ) for some constants M, c > 0 that are independent of  $z_0$ . Finally, we denote by T and T the triangular and prismatic, respectively, sets

$$\mathcal{T} = \left\{ (x, \xi) \in [0, 1]^2 : 0 \le \xi \le x \le 1 \right\},\tag{3a}$$

$$\mathcal{P} = \{ (x, \xi, y) \in [0, 1]^3 : (x, \xi) \in \mathcal{T} \}.$$
 (3b)

# 2. Stabilization of continua $\infty + m$ systems

## 2.1. Continua $\infty + m$ systems of hyperbolic PDEs

The considered class of systems can be thought of as the continuum counterpart of n+m hyperbolic systems in the limit case  $n\to\infty$  (this aspect is considered formally in Sections 4 and 5). However, instead of considering a countably infinite number as  $n\to\infty$ , we replace the n-part by an (uncountably infinite) ensemble over the variable  $y\in[0,1]$ . We note that the class of systems (4), (5) is broader than the one obtained as continuum limit of a respective n+m system (49), (50) in Section 4, as (4), (5) is not limited to countably infinite ensembles. Thus, the considered class of continuum systems is of the form

$$u_{t}(t, x, y) + \lambda(x, y)u_{x}(t, x, y) =$$

$$\int_{0}^{1} \sigma(x, y, \eta)u(t, x, \eta)d\eta + \mathbf{W}(x, y)\mathbf{v}(t, x),$$

$$\mathbf{W}(t, y) - \mathbf{M}(y)\mathbf{v}(t, y) =$$
(4a)

$$\int_0^1 \Theta(x, y) u(t, x, y) dy + \Psi(x) \mathbf{v}(t, x), \tag{4b}$$

with boundary conditions

$$u(t,0,y) = \mathbf{Q}(y)\mathbf{v}(t,0), \tag{5a}$$

$$\mathbf{v}(t,1) = \mathbf{U}(t),\tag{5b}$$

for almost every  $y \in [0, 1]$ . Here we employ the matrix notation for  $\mathbf{v}, \mathbf{U}, \mathbf{M}, \boldsymbol{\Theta}, \boldsymbol{\Psi}, \mathbf{W}$ , and  $\mathbf{Q}$  for the sake of conciseness, that is,  $\mathbf{v} = \begin{pmatrix} v^j \end{pmatrix}_{j=1}^m, \mathbf{U} = \begin{pmatrix} U^j \end{pmatrix}_{j=1}^m$ , and the parameters are as follows.

**Assumption 1.** The parameters of (4), (5) are such that

$$\mathbf{M} = \text{diag}(\mu_i)_{i=1}^m \in C^1([0, 1]; \mathbb{R}^{m \times m}), \tag{6a}$$

$$\Theta = (\theta_j)_{i=1}^m \in C([0, 1]; L^2([0, 1]; \mathbb{R}^m)), \tag{6b}$$

$$\Psi = (\psi_{i,j})_{i,i-1}^m \in C([0,1]; \mathbb{R}^{m \times m}), \tag{6c}$$

$$\mathbf{W} = \begin{bmatrix} W_1 & \cdots & W_m \end{bmatrix} \in C([0, 1]; L^2([0, 1]; \mathbb{R}^{1 \times m})), \tag{6d}$$

$$\mathbf{Q} = \begin{bmatrix} Q_1 & \cdots & Q_m \end{bmatrix} \in L^2([0, 1]; \mathbb{R}^{1 \times m}), \tag{6e}$$

with  $\lambda \in C^1([0, 1]^2; \mathbb{R})$  and  $\sigma \in C([0, 1]; L^2([0, 1]^2; \mathbb{R}))$ . Moreover,  $\lambda(x, y) > 0$  for all  $x, y \in [0, 1]$  and

$$\mu_1(x) > \mu_2(x) > \dots > \mu_m(x) > 0,$$
 (7)

for all  $x \in [0, 1]$ . Finally,  $\psi_{i,j} = 0$  for all j = 1, ..., m.

**Remark 1.** Under Assumption 1, it can be shown by using the same arguments as in Humaloja and Bekiaris-Liberis (2025b, Prop. B.1) that the system (4), (5) is well-posed on  $E_c$ . That is, for any initial conditions  $u_0 \in L^2([0,1];L^2([0,1];\mathbb{R}))$ ,  $\mathbf{v}_0 \in L^2([0,1];\mathbb{R}^m)$  and input  $\mathbf{U} \in L^2_{loc}([0,+\infty);\mathbb{R}^m)$ , there is a unique (weak) solution to (4), (5) satisfying  $(u,\mathbf{v}) \in C([0,+\infty);E_c)$ .

#### 2.2. Continuum backstepping kernel equations

The target system for the continuum Volterra backstepping transformation is essentially chosen as the  $n \to \infty$  continuum counterpart of the respective n+m target system in Hu et al. (2016, Sect. III.A), i.e.,

$$\alpha_{t}(t, x, y) + \lambda(x, y)\alpha_{x}(t, x, y) =$$

$$\int_{0}^{1} \sigma(x, y, \eta)\alpha(t, x, \eta)d\eta + \mathbf{W}(x, y)\boldsymbol{\beta}(t, x)$$

$$+ \int_{0}^{1} \int_{0}^{x} C^{+}(x, \xi, y, \eta)\alpha(t, \xi, \eta)d\xi d\eta$$

$$+ \int_{0}^{x} \mathbf{C}^{-}(x, \xi, y)\boldsymbol{\beta}(t, \xi)d\xi, \tag{8a}$$

with boundary conditions

$$\alpha(t, 0, y) = \mathbf{Q}(y)\boldsymbol{\beta}(t, 0), \tag{9a}$$

$$\boldsymbol{\beta}(t,1) = \mathbf{0},\tag{9b}$$

 $\boldsymbol{\beta}_t(t,x) - \mathbf{M}(x)\boldsymbol{\beta}_x(t,x) = \mathbf{G}(x)\boldsymbol{\beta}(t,0),$ 

(8b)

for (almost) all  $y \in [0, 1]$ , where  $C^+ \in L^{\infty}(\mathcal{T}; L^2([0, 1]^2; \mathbb{R}))$ ,  $\mathbf{C}^- \in L^{\infty}(\mathcal{T}; L^2([0, 1]; \mathbb{R}^{1 \times m}))$ , and  $\mathbf{G} \in L^{\infty}([0, 1]; \mathbb{R}^{m \times m})$  is of the form

$$\mathbf{G}(x) = \begin{bmatrix} 0 & \cdots & \cdots & 0 \\ G_{2,1}(x) & \ddots & \ddots & \vdots \\ \vdots & \ddots & \ddots & \vdots \\ G_{m,1}(x) & \cdots & G_{m,m-1}(x) & 0 \end{bmatrix}.$$
 (10)

The choice of the target system (8), (9) is guided by the fact that the  $\beta$ -part is decoupled from the  $\alpha$ -part and, similarly to the n+m case, tends to zero in finite time. Consequently, the remaining

<sup>&</sup>lt;sup>1</sup> This comes without loss of generality, as such terms can be removed using a change of variables (see also, e.g., Hu et al. (2016, 2019)).

dynamics for  $\alpha$  are exponentially stable analogously to Alleaume and Krstic (2025, (33), (34)). In order to map (4), (5) into (8), (9), we employ the following continuum Volterra transformation

$$\alpha(t, x, y) = u(t, x, y)$$

$$\beta(t, x) = \mathbf{v}(t, x) - \int_0^x \mathbf{L}(x, \xi) \mathbf{v}(t, \xi) d\xi$$

$$- \int_0^x \int_0^1 \mathbf{K}(x, \xi, y) u(t, \xi, y) dy d\xi,$$
(11a)

where  $\mathbf{L} \in L^{\infty}(\mathcal{T}; \mathbb{R}^{m \times m})$  and  $\mathbf{K} \in L^{\infty}(\mathcal{T}; L^2([0, 1]; \mathbb{R}^m))$  are the backstepping kernels. We note that (11b) comprises a Volterra integral operator applied to the inner product in  $E_c$  of  $(\mathbf{K}, \mathbf{L})$  and  $(u, \mathbf{v})$ .

Derivation of the continuum kernels equations is provided in Appendix A. We obtain that  $\bf L$  and  $\bf K$  need to satisfy the following kernel equations

$$\mathbf{M}(x)\mathbf{K}_{x}(x,\xi,y) - \mathbf{K}_{\varepsilon}(x,\xi,y)\lambda(\xi,y) - \mathbf{K}(x,\xi,y)\lambda_{\varepsilon}(\xi,y) =$$

$$\mathbf{L}(x,\xi)\Theta(\xi,y) + \int_0^1 \mathbf{K}(x,\xi,\eta)\sigma(\xi,\eta,y)d\eta, \quad (12a)$$

$$\mathbf{M}(x)\mathbf{L}_{x}(x,\xi) + \mathbf{L}_{\xi}(x,\xi)\mathbf{M}(\xi) + \mathbf{L}(x,\xi)\mathbf{M}'(\xi) =$$

$$\mathbf{L}(x,\xi)\Psi(\xi) + \int_0^1 \mathbf{K}(x,\xi,y)\mathbf{W}(\xi,y)dy, \qquad (12b)$$

with boundary conditions

$$\mathbf{M}(x)\mathbf{L}(x,x) - \mathbf{L}(x,x)\mathbf{M}(x) + \mathbf{\Psi}(x) = 0, \tag{13a}$$

$$\mathbf{K}(x, x, y)\lambda(x, y) + \mathbf{M}(x)\mathbf{K}(x, x, y) + \Theta(x, y) = 0,$$
(13b)

$$\mathbf{L}(x,0)\mathbf{M}(0) - \int_{0}^{1} \mathbf{K}(x,0,y)\lambda(0,y)\mathbf{Q}(y)dy = \mathbf{G}(x),$$
 (13c)

for almost all  $0 \le \xi \le x \le 1$  and  $y \in [0, 1]$ . More precisely, (13c) splits into two parts, for  $i \le j$  and i > j, respectively,

$$L_{i,j}(x,0) = \frac{1}{\mu_i(0)} \int_0^1 K_i(x,0,y) \lambda(0,y) Q_j(y) dy,$$
 (14a)

$$G_{i,j}(x) = L_{i,j}(x,0)\mu_j(0) - \int_0^1 K_i(x,0,y)\lambda(0,y)Q_j(y)dy, \qquad (14b)$$

where (14a) acts as a boundary condition for (12) and (14b) defines the nonzero elements of **G** shown in (10). Similarly to Hu et al. (2016, 2019), we also impose additional, artificial boundary conditions, to ensure the well-posedness of the kernel equations, as follows

$$\forall j < i: L_{i,j}(1,\xi) = l_{i,j}^{(1)}(\xi),$$
 (15)

where the functions  $l_{i,j}^{(1)}$  are chosen such that a  $C^0$  compatibility condition<sup>2</sup> is satisfied on  $(x, \xi) = (1, 1)$ . Thus, consistently with (13a), we impose

$$l_{i,j}^{(1)}(1) = -\frac{\psi_{i,j}(1)}{\mu_i(1) - \mu_i(1)},\tag{16}$$

for all j < i. The well-posedness of the kernel equations (12)–(16) is considered in Section 3.

#### 2.3. Backstepping feedback law and stability result

The backstepping control law for j = 1, ..., m is given by

$$U^{j}(t) = \int_{0}^{1} \int_{0}^{1} K_{j}(1, \xi, y) u(t, \xi, y) dy d\xi + \int_{0}^{1} \sum_{i=1}^{m} L_{j,i}(1, \xi) v^{i}(t, \xi) d\xi,$$
(17)

which stabilizes (4), (5) by Theorem 1.

**Theorem 1.** Under Assumption 1, the control law (17) exponentially stabilizes the system (4), (5) on  $E_c$ .

**Proof.** Well-Posedness: We first establish that the target system (8), (9) has a well-posed solution on  $E_c$ , which we achieve by utilizing feedback results for the well-posed system (4), (5) (see Remark 1). By Tucsnak and Weiss (2009, Sect. 10.1), we can express the well-posed, boundary-controlled PDE (4), (5) as a well-posed abstract Cauchy problem  $\dot{z}(t) = Az(t) + BU(t)$  on the Hilbert space  $E_c$ , where  $z = (u, \mathbf{v})$ , the system  $\dot{z}(t) = Az(t)$ corresponds to (4) with the homogeneous boundary condition from (5) through the domain of A, and BU(t) corresponds to the boundary control in (5). (We skip the explicit expressions of A and B as knowing that they exist suffices here.) Now, expressing the backstepping control law (17) as U(t) = Fz(t), the closedloop dynamics of (4), (5) under the control law (17) are given by  $\dot{z}(t) = (A + BF)z(t)$ . As F is a bounded linear operator from  $E_c$  to  $\mathbb{R}^m$ , the operator A + BF is the generator of a strongly continuous semigroup by Tucsnak and Weiss (2009, Cor. 5.5.1), and hence, the dynamics  $\dot{z}(t) = (A+BF)z(t)$  have a well-posed solution on  $E_c$ . Now, by applying the linear, bounded state transformation (11) (see Theorem 2 in Section 3), we have that the target system (8), (9) has a well-posed solution on  $E_c$  as well.

Lyapunov Stability: Now we show that the (weak; see Humaloja and Bekiaris-Liberis (2025b, Rem. C.1) for details on the fact that existence and uniqueness of a weak solution suffices for making our Lyapunov-based arguments legitimate) solution to (8), (9) decays exponentially to zero, which by the invertibility of the transform (11) (see Lemma 8 in Appendix B) implies that the system (4), (5) under the control law (17) is exponentially stable. Inspired by Hu et al. (2019, Prop. 2.1), the candidate Lyapunov functional with parameters  $\delta$ ,  $\mathbf{D} = \mathrm{diag}(D_1, \ldots, D_m) > 0$  is taken as

$$V(t) = \int_0^1 \int_0^1 e^{-\delta x} \frac{\alpha^2(t, x, y)}{\lambda(x, y)} dy dx$$
$$+ \int_0^1 e^{\delta x} \boldsymbol{\beta}^T(t, x) \mathbf{D} \mathbf{M}^{-1}(x) \boldsymbol{\beta}(t, x) dx.$$
(18)

Computing  $\dot{V}(t)$  and integrating by parts in x gives

$$\begin{split} \dot{V}(t) &= \left[ -e^{-\delta x} \|\alpha(t,x,\cdot)\|_{L^{2}}^{2} + e^{\delta x} \|\pmb{\beta}(t,x)\|_{\mathbf{D}}^{2} \right]_{0}^{1} \\ &- \delta \int_{0}^{1} \left( e^{-\delta x} \|\alpha(t,x,\cdot)\|_{L^{2}}^{2} + e^{\delta x} \|\pmb{\beta}(t,x)\|_{\mathbf{D}}^{2} \right) dx \\ &+ 2 \int_{0}^{1} \int_{0}^{1} \int_{0}^{1} e^{-\delta x} \frac{\alpha(t,x,y)}{\lambda(x,y)} \sigma(x,y,\eta) \alpha(t,x,\eta) d\eta dy dx \\ &+ 2 \int_{0}^{1} \int_{0}^{1} e^{-\delta x} \frac{\alpha(t,x,y)}{\lambda(x,y)} \mathbf{W}(x,y) \pmb{\beta}(t,x) dy dx \\ &+ 2 \int_{0}^{1} \int_{0}^{1} \int_{0}^{1} \int_{0}^{x} e^{-\delta x} \frac{\alpha(t,x,y)}{\lambda(x,y)} C^{+}(x,\xi,y,\eta) \alpha(t,\xi,\eta) d\xi d\eta dy dx \\ &+ 2 \int_{0}^{1} \int_{0}^{1} \int_{0}^{x} e^{-\delta x} \frac{\alpha(t,x,y)}{\lambda(x,y)} C^{-}(x,\xi,y) \pmb{\beta}(t,\xi) d\xi dy dx \end{split}$$

<sup>&</sup>lt;sup>2</sup> While  $C^2$  compatibility conditions (and higher regularity of parameters) are sought in Hu et al. (2019) for obtaining (piecewise)  $C^2$  kernels, for our purposes  $C^0$  compatibility conditions are enough.

<sup>&</sup>lt;sup>3</sup> For the **L** kernels, a compatibility condition cannot (generally) be satisfied on  $(x, \xi) = (0, 0)$  due to (13a) and (13c), (13b).

$$+ \int_{0}^{1} e^{\delta x} \boldsymbol{\beta}^{T}(t, x) \left( \mathbf{D} \mathbf{M}^{-1}(x) \mathbf{G}(x) + \mathbf{G}^{T}(x) \mathbf{M}^{-1}(x) \mathbf{D} \right) \boldsymbol{\beta}(t, 0) dx,$$
(19)

where  $\|\cdot\|_{\mathbf{D}}^2 = \langle\cdot,\mathbf{D}\cdot\rangle_{\mathbb{R}^m}$  denotes the **D**-weighted inner product. Using the following bounds (that exist by Assumption 1 using Theorem 2 and Lemma 7 in Appendix A)

$$m_{\lambda} = \min_{x,y \in [0,1]} \lambda(x,y), \tag{20a}$$

$$m_{\mu} = \min_{i \in \{1, \dots, m\}} \min_{x \in \{0, 1\}} \mu_{j}(x),$$
 (20b)

$$M_{\sigma} = \max_{x \in [0,1]} \left\| \int_{0}^{1} \sigma(x, \cdot, \eta) d\eta \right\|_{L^{2}}, \tag{20c}$$

$$M_W = \max_{j=1,\dots,m} \max_{x \in [0,1]} \|W_j(x,\cdot)\|_{L^2}, \tag{20d}$$

$$M_{C^{+}} = \underset{(x,\xi) \in \mathcal{T}}{\text{esssup}} \left\| \int_{0}^{1} C^{+}(x,\xi,\cdot,\eta) d\eta \right\|_{L^{2}}, \tag{20e}$$

$$M_{C^{-}} = \max_{j \in \{1, \dots, m\}} \underset{(x, \xi) \in \mathcal{T}}{\text{esssup}} \| C_{j}^{-}(x, \xi, \cdot) \|_{L^{2}}, \tag{20f}$$

$$M_G = \max_{i,j \in \{1,...,m\}} \underset{x \in [0,1]}{\text{esssup}} \left| G_{ij}(x) \right|, \tag{20g}$$

$$M_Q = \max_{j=1,\dots,m} \|Q_j\|_{L^2},\tag{20h}$$

the boundary conditions (9), the Cauchy–Schwarz inequality, and  $2 \langle f,g \rangle_{L^2} \leq \|f\|_{L^2}^2 + \|g\|_{L^2}^2$  for any  $f,g \in L^2$ , we can estimate (19) as  $^4$ 

$$\dot{V}(t) \leq -\boldsymbol{\beta}^{T}(t,0) \left(\mathbf{D} - M_{Q}^{2}I_{m\times m}\right) \boldsymbol{\beta}(t,0) 
- \delta \int_{0}^{1} \left(e^{-\delta x} \|\alpha(t,x,\cdot)\|_{L^{2}}^{2} + e^{\delta x} \|\boldsymbol{\beta}(t,x)\|_{\mathbf{D}}^{2}\right) dx 
+ 2 \int_{0}^{1} e^{-\delta x} \frac{M_{\sigma} + M_{C^{+}}}{m_{\lambda}} \|\alpha(t,x,\cdot)\|_{L^{2}}^{2} dx 
+ \int_{0}^{1} e^{-\delta x} \left(\frac{\|\alpha(t,x,\cdot)\|_{L^{2}}^{2}}{m_{\lambda}^{2}} + M_{W}^{2} \|\boldsymbol{\beta}(t,x)\|_{\mathbb{R}^{m}}^{2}\right) dx 
+ \int_{0}^{1} e^{-\delta x} \left(\frac{\|\alpha(t,x,\cdot)\|_{L^{2}}^{2}}{m_{\lambda}^{2}} + M_{C^{-}}^{2} \|\boldsymbol{\beta}(t,x)\|_{\mathbb{R}^{m}}^{2}\right) dx 
+ mM_{G} \int_{0}^{1} e^{\delta x} \boldsymbol{\beta}^{T}(t,x) \mathbf{D} \mathbf{M}^{-1}(x) \boldsymbol{\beta}(t,x) dx 
+ \frac{mM_{G} e^{\delta}}{\delta m_{u}} \boldsymbol{\beta}^{T}(t,0) \mathbf{F} \boldsymbol{\beta}(t,0), \tag{21}$$

where  $\mathbf{F} = \operatorname{diag}(F_1, \dots, F_m)$  with

$$F_{j} = \begin{cases} \sum_{i=j+1}^{m} D_{i}, & 1 \le j \le m-1, \\ 0, & j=m, \end{cases}$$
 (22)

where we employ the lower-triangular structure of **G** given in (10) on the last two lines of (21). Now,  $\dot{V}(t)$  can be guaranteed to be negative definite by choosing  $\delta$  and **D** such that

$$\delta > \max \left\{ \frac{2m_{\lambda}(M_{\sigma} + M_{C^{+}}) + 2}{m_{\lambda}^{2}}, \frac{M_{W}^{2} + M_{C^{-}}^{2} + mM_{G}}{m_{\mu}} \right\},$$
(23a)

$$D_{j} > \begin{cases} \max \left\{ M_{Q}^{2}, 1 \right\}, & j = m, \\ \max \left\{ M_{Q}^{2}, 1 \right\} + \frac{m M_{Q} e^{\delta}}{\delta m_{\mu}} \sum_{i=j+1}^{m} D_{i}, & j < m. \end{cases}$$
 (23b)

More specifically, by defining

$$c_{V} = \delta - \max \left\{ \frac{2m_{\lambda}(M_{\sigma} + M_{C^{+}}) + 2}{m_{\lambda}^{2}}, \frac{M_{W}^{2} + M_{C^{-}}^{2} + mM_{G}}{m_{\mu}} \right\},$$
(24)

we have

$$\dot{V}(t) \le -\frac{c_V}{\max\left\{M_{\mu}, M_{\lambda}\right\}} V(t),\tag{25}$$

where

$$M_{\lambda} = \max_{x,y \in [0,1]} \lambda(x,y), \quad M_{\mu} = \max_{j=\{1,\dots,m\}} \max_{x \in [0,1]} \mu_j(x),$$
 (26)

which shows that the target system (8), (9) is exponentially stable. Thus, due to the invertibility of the transform (11) established in Lemma 8 in Appendix B, the control law (17) exponentially stabilizes (4), (5).  $\Box$ 

#### 3. Well-posedness of the continuum kernels

**Theorem 2.** Under Assumption 1, the continuum kernel equations (12)–(16) have a well-posed solution  $\mathbf{K} \in L^{\infty}(\mathcal{T}; L^2([0, 1]; \mathbb{R}^m))$  and  $\mathbf{L} \in L^{\infty}(\mathcal{T}; \mathbb{R}^{m \times m})$ . Moreover, the solution is piecewise continuous in  $(x, \xi) \in \mathcal{T}$ , where the set of discontinuities comprises finitely many continuously differentiable, monotone curves.

The proof is presented at the end of this section by utilizing the following lemmas. First, the kernels are split into subdomains to deal with the potential discontinuity in the  $L_{i,j}$  kernels for i < j stemming from  $(x, \xi) = (0, 0)$  due to the boundary conditions (13a) and (13c), (13b). Once the kernels are split into subdomains, the resulting kernel equations can be solved by transforming them into integral equations along the characteristic curves and solving these integral equations by using the method of successive approximations combining Alleaume and Krstic (2025, Sect. VI) and Hu et al. (2016, Sect. VI). In particular, we need to ensure continuity of the characteristic curves such that the successive approximations for the  $K_i$  kernels, for  $i = 1, \ldots, m$ , are  $L^2$  in y for almost all  $(x, \xi) \in \mathcal{T}$ .

**Lemma 1** (Splitting the Kernels into Subdomains of Continuity). The kernel equations (12) can be equivalently written in  $L^{\infty}(\mathcal{T}; L^2([0, 1]; \mathbb{R}^m) \times \mathbb{R}^{m \times m})$  as

$$\mu_{i}(x)\partial_{x}K_{i}^{p}(x,\xi,y) - \partial_{\xi}K_{i}^{p}(x,\xi,y)\lambda(\xi,y) - K_{i}^{p}(x,\xi,y)\lambda_{\xi}(\xi,y) =$$

$$\sum_{\ell=1}^{m} L_{i,\ell}^{p}(x,\xi)\theta_{\ell}(\xi,y) + \int_{0}^{1} K_{i}^{p}(x,\xi,\eta)\sigma(\xi,\eta,y)d\eta,$$

$$(27a)$$

$$\mu_{i}(x)\partial_{x}L_{i,j}^{p}(x,\xi) + \mu_{j}(\xi)\partial_{\xi}L_{i,j}^{p}(x,\xi) + \mu'_{j}(\xi)L_{i,j}^{p}(x,\xi) =$$

$$\sum_{\ell=1}^{m} L_{i,\ell}^{p}(x,\xi)\psi_{\ell,j}(\xi) + \int_{0}^{1} K_{i}^{p}(x,\xi,y)W_{j}(\xi,y)dy,$$

$$(27b)$$

for  $1 \leq i \leq p \leq m$  and  $j = 1, \ldots, m$ , where  $L_{i,j}^p, K_i^p$  denote the restrictions of the kernels to  $\mathcal{T}_i^p$  and  $\mathcal{P}_i^p$ , respectively, defined as

$$\mathcal{T}_{i}^{p} = \left\{ (x, \xi) \in [0, 1]^{2} : \rho_{i}^{p+1}(x) \le \xi \le \rho_{i}^{p}(x) \right\}, \tag{28a}$$

$$\mathcal{P}_{i}^{p} = \left\{ (x, \xi, y) \in [0, 1]^{3} : (x, \xi) \in \mathcal{T}_{i}^{p} \right\}, \tag{28b}$$

where  $\rho_i^{m+1} = 0$  for all i = 1, ..., m and

$$\rho_i^p(x) = \phi_n^{-1}(\phi_i(x)), \tag{29}$$

<sup>&</sup>lt;sup>4</sup> We use the shorthand notation  $\|\alpha(t,x,\cdot)\|_{L^2}$  instead of writing the integrals over y explicitly. While this is a slight abuse of notation (as  $\alpha(t,x,\cdot)$  is not necessarily in  $L^2$ ), these expressions are valid appearing inside the integrals over x

<sup>5</sup> for 1 < i < p < m with

$$\phi_i(x) = \int_0^x \frac{ds}{\mu_i(s)}, \qquad i = 1, \dots, m.$$
 (30)

The boundary conditions for (27) are given by

$$\forall j \neq i: \qquad L_{i,j}^{i}(x,x) = -\frac{\psi_{i,j}(x)}{\mu_{i}(x) - \mu_{j}(x)},$$

$$\forall i: \quad K_{i}^{i}(x,x,y) = -\frac{\theta_{i}(x,y)}{\lambda(x,y) + \mu_{i}(x)},$$
(31a)

$$\forall i: \quad K_i^i(x, x, y) = -\frac{\theta_i(x, y)}{\lambda(x, y) + \mu_i(x)},\tag{31b}$$

$$\forall i \leq j: \qquad L_{i,j}^{m}(x,0) = \frac{1}{\mu_{j}(0)} \int_{0}^{1} K_{i}^{m}(x,0,y) \lambda(0,y) Q_{j}(y) dy, \tag{31c}$$

for i, j = 1, ..., m, with the artificial boundary conditions

$$L_{ij}^{p}(1,\xi) = l_{i,j}^{(1)}(\xi), \tag{32}$$

for all  $\xi \in [\rho_i^{p+1}(1), \rho_i^p(1)]$ ,  $p = i, \ldots, m$ , and  $1 \le j < i \le m$ . Moreover, the segmented kernels  $K_i^p$ ,  $L_{i,j}^p$  are subject to continuity conditions

$$\forall i < p, \forall j \neq p:$$
  $L_{i,i}^{p-1}(x, \rho_i^p(x)) = L_{i,i}^p(x, \rho_i^p(x)),$  (33a)

$$\forall i < p:$$
  $K_i^{p-1}(x, \rho_i^p(x), y) = K_i^p(x, \rho_i^p(x), y),$  (33b)

for all i, j = 1, ..., m,  $i , and <math>x, y \in [0, 1]$ .

**Proof.** After splitting the kernels into the  $\mathcal{T}_i^p$  and  $\mathcal{P}_i^p$  segments, the transformation (11b) can be rewritten componentwise for  $i = 1, \ldots, m$  as

$$\beta_{i}(t,x) = v_{i}(t,x) - \sum_{j=1}^{m} \sum_{p=i}^{m} \int_{\rho_{i}^{p+1}(x)}^{\rho_{i}^{p}(x)} L_{i,j}^{p}(x,\xi) v_{j}(t,\xi) d\xi$$

$$- \sum_{p=i}^{m} \int_{\rho_{i}^{p+1}(x)}^{\rho_{i}^{p}(x)} \int_{0}^{1} K_{i}^{p}(x,\xi,y) u(t,\xi,y) dy d\xi.$$
(34)

The kernel equations (27) are obtained by inserting (34) to (8b) and integrating by parts once (similarly to Appendix A). In fact, the kernel equations (27) are exactly of the same form as (12) (written componentwise), and the boundary conditions (31), (32) correspond to (13a), (13b), (14a), and (15) along the respective boundaries (see Fig. 1 for an illustration of the  $\mathcal{T}_i^p$  segments). Thus, the only difference to (12)-(15) are the continuity conditions (33), which arise due to the segmentation of  $\mathcal{T}$  when differentiating (34) in x and integrating by parts once.  $\Box$ 

The kernel equations (27) for  $L_{i,j}^p$  and  $K_i^p$  on the segments  $\mathcal{T}_i^p$ and  $\mathcal{P}_{i}^{p}$  with boundary conditions (31)–(33) can be transformed into integral equations. In order to do this, in Lemma 2 we solve the characteristic projections for (27).

**Lemma 2** (Continuity of Characteristic Projections). The characteristic projections for the kernel equations (27) are continuous on  $\mathcal{T}_i^{\mu}$ and  $\mathcal{P}_i^p$  for all  $1 \leq i \leq p \leq m$ .

**Proof.** As  $\lambda$  is assumed to be in  $C^1([0,1]^2;\mathbb{R})$ , we can argue pointwise in  $y \in [0, 1]$  and solve the characteristic projections for the  $K_i^p$  kernels from the following Cauchy problems on  $s \in$  $[0, s_{i,p}^f(y)]$  for arbitrary, fixed  $y \in [0, 1]$  and  $1 \le i \le p \le m$ 

$$\frac{d}{ds}\hat{x}_{i,p}(s,y) = -\mu_i(\hat{x}_{i,p}(s,y)),\tag{35a}$$

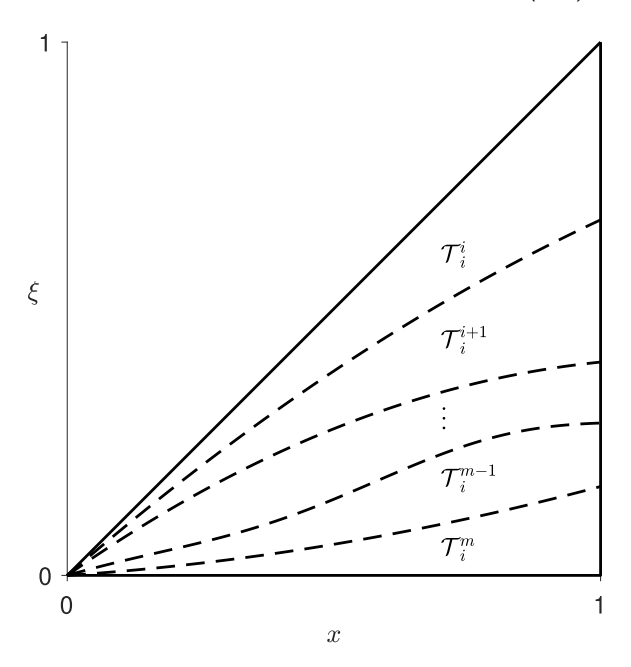


**Fig. 1.** Illustration of the segments  $\mathcal{T}_i^p$  for  $1 \le i \le p \le m$ . The dashed lines are the characteristic curves  $\xi = \rho_i^p(x)$  for i .

$$\frac{d}{ds}\hat{\xi}_{i,p}(s,y) = \lambda(\hat{\xi}_{i,p}(s,y),y),\tag{35b}$$

with boundary conditions  $\hat{x}_{i,p}(0,y) = x, \hat{x}_{i,p}(s_{i,p}^f,y)$  $\hat{x}_{i,p}^f(y), \hat{\xi}_{i,p}(0,y) = \xi, \hat{\xi}_{i,p}\left(s_{i,p}^f,y\right) = \hat{\xi}_{i,p}^f(y)$ . Since  $\mu_i$  and  $\lambda(\cdot,y)$  are continuously differentiable and positive by Assumption 1, (35) has a unique (local in s) solution for any  $(x, \xi) \in \mathcal{T}_i^p$  (and each y) by Picard–Lindelöf theorem (Teschl, 2012, Thm 2.2), where  $\hat{x}_{i,p}$ is strictly decreasing in s and  $\xi_{i,p}$  is strictly increasing in s. Thus, for any initial condition  $(x, \xi) \in \mathcal{T}_i^p$ , the solution to (35) tends towards the boundary  $\xi = \rho_i^p(x)$ , where it terminates at  $s = s_{i,p}^f(y)$ with the terminal condition  $(\hat{x}_{i,p}^f, \hat{\xi}_{i,p}^f)$ , and the corresponding boundary condition is given by (31b) for i = p, or by (33b) for i < pp. Considering that we have only split the domain of the kernel equations in the  $(x, \xi)$  plane, we can employ the same continuity arguments, not only in y but also in x and  $\xi$ , as in Alleaume and Krstic (2025, Lem. 4) on each  $\mathcal{P}_i^p$  for all  $1 \le i \le p \le m$ . Thus, the characteristic projections solving (35) are continuous on each  $\mathcal{P}_{i}^{p}$ , particularly as  $\lambda$  and  $\mu_{i}$  are continuously differentiable by Assumption 1.

The characteristic projections for the  $L_{i,j}^p$  kernels are analogous to the  $\ell_{i,i}^p$  kernels encountered in the n+m case. Thus, this observation allows us to study continuity of the characteristic projections for the  $L_{i,j}^p$  kernels similarly to Hu et al. (2019, Thm A.1) and Hu et al. (2016, Sect. VI.A.2). To elaborate, for all i, j =1, ..., m and p = i, ..., m, the characteristic projections for the  $L_{i,j}^p$  kernels are solutions of the following Cauchy problems on  $s \in [0, s_{i,i,n}^f]$ 

$$\frac{d}{ds}\hat{x}_{i,j,p}(s) = \epsilon_{i,j}\mu_i(\hat{x}_{i,j,p}(s)),\tag{36a}$$

$$\frac{d}{ds}\hat{\xi}_{i,j,p}(s) = \epsilon_{i,j}\mu_j(\hat{\xi}_{i,j,p}(s)),\tag{36b}$$

with boundary conditions  $\hat{x}_{i,j,p}(0) = x, \hat{x}_{i,j,p}(s_{i,j,p}^f) = \hat{x}_{i,j,p}^f$  $\hat{\xi}_{i,j,p}(0) = \xi, \hat{\xi}_{i,j,p}\left(s_{i,j,p}^f\right) = \hat{\xi}_{i,j,p}^f$ , and  $\epsilon_{i,j}$  defined as

$$\epsilon_{i,j} = \begin{cases} 1, & i > j \\ -1, & i \le j. \end{cases} \tag{37}$$

<sup>&</sup>lt;sup>5</sup> These are the characteristic curves of (27b), which are strictly increasing in x and satisfy  $0 = \rho_i^{m+1}(x) < \rho_i^m(x) < \cdots < \rho_i^i(x) = x$  for all  $1 \le i \le m$  and  $x \in (0, 1]$  by (7) (see, e.g., Hu et al. (2019, (A.3))).

For initial condition  $(x, \xi) \in \mathcal{T}_i^p$ , the location of the terminal condition  $(\hat{x}_{i,j,p}^f, \hat{\xi}_{i,j,p}^f)$  depends on i, j and p (cf. Hu et al. (2016, Figs. 4–6)) as follows.

- For i > j, the terminal condition is located either on x = 1 with boundary condition (32) for  $i \le p \le m$ , or on  $\xi = x$  with boundary condition (31a) for p = i, or on  $\xi = \rho_i^p(x)$  with boundary condition (33a) for i .
- For i = j, the terminal condition is located on  $\xi = 0$  for p = m with boundary condition (31c), and on  $\xi = \rho_i^{p+1}(x)$  for  $i \le p < m$  with boundary condition (33a) (for  $p \to p+1$ ).
- For i < j, the terminal condition is located on  $\xi = x$  for p = i with boundary condition (31a), on  $\xi = \rho_i^p(x)$  for  $i with boundary condition (33a), on <math>\xi = 0$  for p = m with boundary condition (31c), and on  $\xi = \rho_i^{p+1}(x)$  for  $j \le p < m$  with boundary condition (33a) (for  $p \to p + 1$ ).

Thus, there exist unique, continuous characteristic projections as the solutions to (36) on  $s \in [0, s_{i,j,p}^f]$ , as every  $\mu_i$  is continuously differentiable by Assumption 1.  $\square$ 

As the final step, we transform the kernel equations (27) into integral equations along the characteristic curves. By virtue of Lemma 2, we can then proceed with the method of successive approximations to obtain the unique continuous kernels  $K_i^p$ ,  $L_{i,j}^p$  solving (27)–(33) on each  $T_i^p$  by Lemma 3. Towards this end, integrating (27) along the characteristic curves and plugging in the boundary conditions (31)–(33) gives

$$K_{i}^{p}(x,\xi,y) - B_{i,p}^{1}\left(x_{i,p}^{f}(y),y\right) =$$

$$-\int_{0}^{s_{i,p}^{f}(y)} \left(K_{i}^{p}\left(\hat{x}_{i,p}(s,y),\hat{\xi}_{i,p}(s,y),y\right)\lambda_{\xi}\left(\hat{\xi}_{i,p}(s,y),y\right)\right)$$

$$+\int_{0}^{1}K_{i}^{p}\left(\hat{x}_{i,p}(s,y),\hat{\xi}_{i,p}(s,y),\eta\right)\sigma\left(\hat{\xi}_{i,p}(s,y),\eta,y\right)d\eta$$

$$+\sum_{\ell=1}^{m}L_{i,\ell}^{p}\left(\hat{x}_{i,j,p}(s),\hat{\xi}_{i,j,p}(s)\right)\theta_{\ell}\left(\hat{\xi}_{i,j,p}(s),y\right)\right)ds, \qquad (38a)$$

$$L_{i,j}^{p}(x,\xi) - B_{i,j,p}^{2}\left(\hat{\star}_{i,j,p}\left(s_{i,j,p}^{f}(s)\right)\right) =$$

$$+\epsilon_{i,j}\int_{0}^{s_{i,j,p}^{f}}\left(\mu_{j}'\left(\hat{\xi}_{i,j,p}(s)\right)L_{i,j}^{p}\left(\hat{x}_{i,j,p}(s),\hat{\xi}_{i,j,p}(s)\right)\right)$$

$$-\int_{0}^{1}K_{i}^{p}\left(\hat{x}_{i,j,p}(s),\hat{\xi}_{i,j,p}(s),y\right)W_{j}\left(\hat{\xi}_{i,j,p}(s),y\right)dy$$

$$-\sum_{\ell=1}^{m}L_{i,\ell}^{p}\left(\hat{x}_{i,j,p}(s),\hat{\xi}_{i,j,p}(s)\right)\psi_{\ell,j}\left(\hat{\xi}_{i,j,p}(s)\right)\right)ds, \qquad (38b)$$

where, for j = 1, ..., m and  $1 \le i \le p \le m$ ,

$$B_{i,p}^{1}(x,y) = \begin{cases} -\frac{\theta_{i}(x,y)}{\lambda(x,y) + \mu_{i}(x)}, & p = i \\ K_{i}^{p-1}(x, \rho_{i}^{p}(x), y), & p > i, \end{cases}$$
(39a)
$$B_{i,j,p}^{2}(\star) = \begin{cases} -\frac{\psi_{i,j}(x)}{\mu_{i}(x) - \mu_{j}(x)}, & p = i, i \neq j \\ \frac{l_{i,j}^{(1)}(\xi)}{\mu_{i}(x) - \mu_{j}(x)}, & p \geq i > j \\ l_{i,j}^{(1)}(\xi), & p \geq i > j \\ l_{i,j}^{p-1}(x, \rho_{i}^{p}(x)), & i$$

denote the boundary conditions according to the terminal conditions of the characteristic projections solved in Lemma 2. The integral form (38) of the kernel equations can then be employed in constructing the series of successive approximations, by first

inserting (arbitrary) initial guesses for  $K_i^p$  and  $L_{i,j}^p$ . The convergence of such successive approximations is established in Lemma 3.

**Lemma 3** (Convergence of Successive Approximations). Let  $j=1,\ldots,m$  and  $1 \leq i \leq p \leq m$  be arbitrary, and denote the sequences of successive approximations for the respective kernels  $K_i^p$  and  $L_{i,j}^p$  corresponding to (38), (39) by  $(K_\ell)_{\ell=0}^\infty$  and  $(L_\ell)_{\ell=0}^\infty$ , respectively, where we initialize  $K_0$  and  $L_0$  to zero. Then, the sequences of successive approximations converge such that

$$\lim_{\ell \to \infty} \max_{(x,\xi) \in \mathcal{T}_i^p} \left\| K_{\ell}(x,\xi,\cdot) - K_i^p(x,\xi,\cdot) \right\|_{L^2} = 0, \tag{40a}$$

$$\lim_{\ell \to \infty} \max_{(x,\xi) \in \mathcal{T}_i^p} \left| L_{\ell}(x,\xi) - L_{i,j}^p(x,\xi) \right| = 0. \tag{40b}$$

**Proof.** Denote the differences of successive approximations by  $\Delta K_\ell = K_{\ell+1} - K_\ell$  and  $\Delta L_\ell = L_{\ell+1} - L_\ell$  for  $\ell \geq 0$ . As  $K_0$  and  $L_0$  were initialized to zero, the terms in the sequences of successive approximations for  $\ell \geq 0$  can be written as

$$K_{\ell} = \sum_{l=0}^{\ell} \Delta K_{l}, \qquad L_{\ell} = \sum_{l=0}^{\ell} \Delta L_{l}. \tag{41}$$

Now, the statement of the lemma is equivalent to the convergence of the series of differences (41) in the stated sense, which follows by showing that  $\Delta K_{\ell}$  and  $\Delta L_{\ell}$ , for any  $\ell \geq 0$ , satisfy<sup>6</sup>

$$\|\Delta K_{\ell}(x,\xi,\cdot)\|_{L^{2}} \leq M \frac{M_{K,L}^{\ell} \left(\phi_{i}(x) - \epsilon \phi_{i}(\xi)\right)^{\ell}}{\ell!},\tag{42a}$$

$$|\Delta L_{\ell}(x,\xi)| \le M \frac{M_{K,L}^{\ell} \left(\phi_{i}(x) - \epsilon \phi_{i}(\xi)\right)^{\ell}}{\ell!},\tag{42b}$$

uniformly on any  $\mathcal{T}_i^p$ , where  $M, M_{K,L} > 0$  are given by

$$M = M_B + (1 + M_Q^1) \max_{x,y \in [0,1]} \max_{j=\{1,\dots,m\}} \frac{\|\theta_j(x,\cdot)\|_{L^2}}{\lambda(x,y) + \mu_j(x)},$$
(43a)

$$M_{K,L} = m(1 + M_Q^1) \left( M_{\lambda}^1 + M_{\sigma}^1 + M_{\theta} \right) M_{\epsilon} + m \left( M_{\mu}^1 + M_W + M_{\psi} \right) M_{\epsilon},$$
(43b)

where  $M_B = \max \{M_B^1, M_B^2\}$  with

$$M_B^1 = \max_{1 \le i \ne j \le m} \max_{x \in [0,1]} \left| \frac{\psi_{i,j}(x)}{\mu_i(x) - \mu_j(x)} \right|, \tag{44a}$$

$$M_B^2 = \max_{1 \le i, i \le m} \max_{\xi \in [0, 1]} \left| \ell_{i,j}^{(1)}(\xi) \right|, \tag{44b}$$

 $M_W$  and  $M_{\lambda}$ ,  $M_{\mu}$  are given by (20d), and (26), respectively,

$$M_{\lambda}^{1} = \max_{x, y \in [0, 1]} |\lambda_{x}(x, y)|, \qquad (45a)$$

$$M_{\mu}^{1} = \max_{j=\{1,\dots,m\}} \max_{x \in [0,1]} \left| \mu_{j}'(x) \right|, \tag{45b}$$

$$M_{\sigma}^{1} = \max_{\mathbf{x} \in [0,1]} \left\| \int_{0}^{1} \sigma(\mathbf{x}, \eta, \cdot) d\eta \right\|_{L^{2}}, \tag{45c}$$

$$M_{\theta} = \sum_{j=1}^{m} \max_{x \in [0,1]} \|\theta_{j}(x, \cdot)\|_{L^{2}}, \tag{45d}$$

$$M_{\psi} = \max_{x \in [0,1]} \|\Psi(x)\|_{1},\tag{45e}$$

$$M_{\mathbb{Q}}^{1} = \max_{j=\{1,\dots,m\}} \max_{y \in [0,1]} \frac{\lambda(0,y)}{\mu_{j}(0)} \|Q_{j}\|_{L^{2}}, \tag{45f}$$

<sup>&</sup>lt;sup>6</sup> Note that the estimates (42) depend on *i*, while the functions  $\phi_i(x) - \epsilon \phi_i(\xi)$  are non-negative for  $(x, \xi) \in \mathcal{T}$ .

where the parameter  $0 < \epsilon < 1$  is chosen such that

$$\max_{1 \le j < i \le m} \max_{x \in [0,1]} \frac{\mu_i(x)}{\mu_j(x)} < \epsilon < 1, \tag{46}$$

<sup>7</sup> and  $M_{\epsilon} = \max\{M_{\lambda,\epsilon}, M_{\mu,\epsilon}^1, M_{\mu,\epsilon}^2\}$  with

$$M_{\lambda,\epsilon} = \max_{i \in \{1,\dots,m\}} \max_{x,y \in [0,1]} \frac{\mu_i(x)}{\mu_i(x) + \epsilon \lambda(x,y)},\tag{47a}$$

$$M_{\mu,\epsilon}^{1} = \max_{1 \le j < i \le m} \max_{x \in [0,1]} \frac{\mu_i(x)}{\epsilon \mu_j(x) - \mu_i(x)},\tag{47b}$$

$$M_{\mu,\epsilon}^2 = \max_{1 \le i \le j \le m} \max_{x \in [0,1]} \frac{\mu_i(x)}{\mu_i(x) - \epsilon \mu_j(x)}.$$
 (47c)

Due to linearity, the integral equations and boundary conditions for  $\Delta K_{\ell}$  and  $\Delta L_{\ell}$  are of the same form as (38) and (39), but with K and L replaced by  $\Delta K_{\ell}$  and  $\Delta L_{\ell}$ . Hence, the estimates (42) can be proved by induction based on (38) and (39). Firstly, the constant M (and the initialization of  $K_0$ ,  $L_0$  to zero) guarantees that the estimates (42) are satisfied for  $\ell = 0$ , and for any arbitrary  $\ell > 0$  we have (42) by the induction assumption. To show that (42) then holds for  $\ell \to \ell + 1$ , we insert the estimates (42), (45), and (20), into the integral equations for  $\Delta K_{\ell}$  and  $\Delta L_{\ell}$ . The following estimates for  $\Phi_i(x, \xi) = \phi_i(x) - \epsilon \phi_i(\xi)$  are key to the induction step, and can be proved analogously to Hu et al. (2016, Lem. 6.2) (see also Coron, Hu, Olive, and Shang (2021, Rem. 3.8)), for all i, j = 1, ..., m, p = i, ..., m, and any  $\ell \ge 0$ 

$$\int_{0}^{s_{i,p}^{f}(y)} \Phi_{i}\left(\hat{x}_{i,p}(s,y), \hat{\xi}_{i,p}(s,y)\right)^{\ell} ds \leq M_{\epsilon} \frac{\Phi_{i}\left(x,\xi\right)^{\ell+1}}{\ell+1},$$

$$\int_{0}^{s_{i,j,p}^{f}} \Phi_{i}\left(\hat{x}_{i,j,p}(s), \hat{\xi}_{i,j,p}(s)\right)^{\ell} ds \leq M_{\epsilon} \frac{\Phi_{i}\left(x,\xi\right)^{\ell+1}}{\ell+1},$$
(48a)

$$\int_{0}^{s_{i,j,p}^{f}} \Phi_{i}\left(\hat{x}_{i,j,p}(s), \hat{\xi}_{i,j,p}(s)\right)^{\ell} ds \leq M_{\epsilon} \frac{\Phi_{i}\left(x,\xi\right)^{\ell+1}}{\ell+1},\tag{48b}$$

where  $(x, \xi) \in \mathcal{T}_i^p$  is the (arbitrary) initial point of the respective characteristic curve on the  $x\xi$ -plane.

Using (48) together with (42) and the induction assumption, the induction step follows after similar computations as in Alleaume and Krstic (2025, Sect. VI.C), albeit some additional care is required due to splitting the domain into the  $\mathcal{T}_i^p$  segments, as some boundary conditions depend on  $\Delta K_{\ell}$  and  $\Delta L_{\ell}$ , which are unknown. However, as the boundary condition for  $\Delta K_{\ell}$  on every  $\mathcal{T}_i^i$  is known (due to (39a)), we can solve (38a) first on every  $\mathcal{T}_i^i$ , and then utilize the obtained values to solve (38a) on  $\mathcal{T}_i^{i+1}$ , and so on, up to  $\mathcal{T}_i^m$  (this process is described in detail in Di Meglio et al. (2018, Sect. 3.2)). As the domain  $\mathcal{T}$  is split into at most m segments, we need to solve (38a) at most mtimes over the different segments to compute the next successive approximation. Hence, an adequate value for  $M_{K,L}$  corresponding to the estimate for  $\Delta K_{\ell}$  would be  $m(M_{\lambda}^1 + M_{\sigma}^1 + M_{\theta})M_{\epsilon}$ , which gives the first term of (43b).

Deriving the estimate for  $\Delta L_{\ell}$  follows similar steps, where we again need to traverse through the segments  $\mathcal{T}_i^p$  (depending also on j) to have known boundary conditions for the integral Eq. (38b). That is, for all  $i \neq j$ , we begin from  $\mathcal{T}_i^i$  with known boundary condition on  $\xi = x$  or x = 1, and then utilize the continuity conditions in (39b) up to  $\mathcal{T}_i^m$  if i > j, or up to  $\mathcal{T}_i^{j-1}$  if i < j. For  $i \le j$ , the remaining segments are reached by beginning from  $\mathcal{T}_i^m$  with the boundary condition on  $\xi=0$ , and then utilizing the continuity conditions up to  $\mathcal{T}_i^j$ . As in the case of  $\Delta K_\ell$ , this results in having to solve (38b) at most m times, which results in the last term of (43b). Moreover, the boundary condition on  $\xi = 0$ depends on  $\Delta K_{\ell}$ , which can be dealt with using the estimate derived in the previous paragraph, which results in the remaining term  $mM_0^1(M_\lambda^1 + M_\sigma^1 + M_\theta)M_\epsilon$  in (43b). Thus, the estimate (42)

follows by induction. Hence the series (41) and, equivalently, the sequences of successive approximations converge in the stated sense (40).

**Proof of Theorem 2.** By Lemma 3, the sequences of successive approximations for any  $K_i^p$  and  $L_{i,j}^p$  converge uniformly on  $\mathcal{T}_i^p$  ( $K_i^p$  in the  $L^2$  sense in y), which shows the existence (and well-posedness) of the solutions  $K_i^p$ ,  $L_{i,j}^p$  to the kernel equations (27)–(33). To conclude the proof of Theorem 2, we note that any two  $\mathcal{T}_i^p$  and  $\mathcal{T}_i^s$  with  $p \neq s$  may only intersect along a common boundary  $\xi = \rho_j^r(x)$  for r = p or r = s (if the segments are adjacent), which is a continuously differentiable curve. Thus, as the kernels  $L_{i,j}^p$  and  $K_i^p$  are continuous on each  $(x, \xi) \in \mathcal{T}_i^p$ , and the intersections of these segments comprise a finite number of continuously differentiable curves, the discontinuities of the kernels  $K_i$  and  $L_{i,j}$  may only occur on finitely many continuously differentiable curves, which are additionally monotone.8 In particular, the kernels  $K_i$ ,  $L_{i,j}$  solving (12)–(16) are uniquely determined by  $K_i^p$ ,  $L_{i,i}^p$ , almost everywhere on  $\mathcal{T}$  and  $\mathcal{P}$ .

## 4. Stabilization of large-scale n + m systems by continuum kernels

In this section, we construct a stabilizing control law for largescale n+m systems based on the  $\infty+m$  continuum kernels. The core idea is to establish that, for large n, the exact control kernels constructed based on the n + m system (see Appendix C) can be approximated to any desired accuracy by the continuum kernels computed on the basis of the  $\infty + m$  system.

4.1. Large-scale n + m systems of hyperbolic PDEs

Consider a system of n + m hyperbolic PDEs<sup>9</sup>

$$\mathbf{u}_{t}(t,x) + \mathbf{\Lambda}(x)\mathbf{u}_{x}(t,x) = \frac{1}{n}\mathbf{\Sigma}(x)\mathbf{u}(t,x) + \mathbf{W}(x)\mathbf{v}(t,x), \tag{49a}$$

$$\mathbf{u}_{t}(t,x) + \mathbf{\Lambda}(x)\mathbf{u}_{x}(t,x) = \frac{1}{n}\mathbf{\Sigma}(x)\mathbf{u}(t,x) + \mathbf{W}(x)\mathbf{v}(t,x),$$
(49a)  
$$\mathbf{v}_{t}(t,x) - \mathbf{M}(x)\mathbf{v}_{x}(t,x) = \frac{1}{n}\Theta(x)\mathbf{u}(t,x) + \mathbf{\Psi}(x)\mathbf{v}(t,x),$$
(49b)

with boundary conditions

$$\mathbf{u}(t,0) = \mathbf{Q}\mathbf{v}(t,0), \mathbf{v}(t,1) = \mathbf{U}(t), \tag{50}$$

where  $\Lambda(x) = \text{diag}(\lambda_1(x), \dots, \lambda_n(x)), \Sigma(x) = (\sigma_{i,j}(x))_{i,j=1}^n, \mathbf{W}(x) =$  $(w_{i,j}(x))_{i=1,j=1}^{n}$ ,  $\Theta(x) = (\theta_{j,i}(x))_{j=1,i=1}^{m}$ ,  $\mathbf{Q} = (q_{i,j})_{i=1,j=1}^{n}$ ,  $\mathbf{u} = (u^{i})_{i=1}^{n}$ , and  $\mathbf{M}$ ,  $\Psi$  correspond to the respective parameters in (4b). As in Anfinsen and Aamo (2019), Auriol and Di Meglio (2016) and Hu et al. (2016, 2019), we make the following assumptions on the parameters.

**Assumption 2.** The transport velocities in (49) are continuously differentiable with  $\lambda_i(x) > 0$  for all  $x \in [0, 1]$  and i = 1, ..., n, and  $\mu_j$  satisfying (7). The parameters  $\Sigma, \mathbf{W}, \Theta, \Psi$  are continuous with  $\psi_{i,j} = 0$  for all  $j = 1, \ldots, m$ .

Remark 2. Under Assumption 2, it can be shown by using the same arguments as in Humaloja and Bekiaris-Liberis (2025b, Prop. A.1) that the system (49), (50) is well-posed on the Hilbert space E.

<sup>7</sup> Such  $\epsilon$  exist by (7).

In fact, the discontinuities may only occur in the  $L_{i,j}$  kernels for  $1 \leq i < j$  $j \le m$  along the curves  $\xi = \rho_i^j(x)$  due to (33).

<sup>&</sup>lt;sup>9</sup> We scale the sums involving the *n*-part states  $u^i, i=1,\ldots,n$  by 1/n in order to make the considerations in the limit  $n o \infty$  more natural, as discussed in Humaloja and Bekiaris-Liberis (2025b, Rem. 2.2). Thus, under continuity of the continuum parameters and (51), e.g., the sum/vector  $\frac{1}{n}\Theta(x)\mathbf{u}(t,x)$  tends to

 $<sup>\</sup>oint \Theta(x,y)u(t,x,y)dy$  as  $n \to \infty$  (provided that **u** and u are also connected appropriately, as in Theorem 4).

#### 4.2. Control design and stability result

Consider any continuous functions  $\theta_j$ ,  $W_j$ ,  $Q_j$ ,  $\lambda$ , and  $\sigma$  satisfying Assumption 1 with

$$\theta_i(x, i/n) = \theta_{i,i}(x), \tag{51a}$$

$$W_i(x, i/n) = w_{i,j}(x), \tag{51b}$$

$$Q_i(i/n) = q_{i,i}, (51c)$$

$$\lambda(x, i/n) = \lambda_i(x), \tag{51d}$$

$$\sigma(x, i/n, l/n) = \sigma_{i,l}(x), \tag{51e}$$

for all  $x \in [0, 1]$ , i, l = 1, ..., n and j = 1, ..., m. It follows by Theorem 2 that the corresponding continuum kernel equations (27)–(33) have well-posed solution  $K_i^p \in C(\mathcal{T}_i^p; L^2([0, 1]; \mathbb{R}))$ ,  $L_{i,j}^p \in C(\mathcal{T}_i^p; \mathbb{R})$  for all j = 1, ..., m and  $1 \le i \le p \le m$ . Thus, construct the following functions for all  $(x, \xi) \in \mathcal{T}_i^p$  with  $1 \le i \le p \le m$ , 10

$$\widetilde{K}_{i,l}^{p}(x,\xi) = n \int_{(l-1)/n}^{l/n} K_{i}^{p}(x,\xi,y) dy, \quad l = 1, \dots, n,$$
 (52a)

$$\widetilde{\ell}_{i,j}^p(x,\xi) = L_{i,j}^p(x,\xi), \quad j = 1, \dots, m.$$
(52b)

We have the following stabilization result.

**Theorem 3.** Consider (49), (50) satisfying Assumption 2. Let (continuum) parameters  $\theta_j$ ,  $W_j$ ,  $Q_j$  for j = 1, ..., m and  $\sigma$ ,  $\lambda$  satisfy Assumption 1 and relations (51). Define the feedback laws

$$U^{i}(t) = \sum_{l=1}^{n} \sum_{p=i}^{m} \int_{\rho_{i}^{p+1}(1)}^{\rho_{i}^{p}(1)} \frac{1}{n} \widetilde{k}_{i,l}^{p}(1,\xi) u^{l}(t,\xi) d\xi + \sum_{i=1}^{m} \sum_{p=i}^{m} \int_{\rho_{i}^{p}(1)}^{\rho_{i}^{p}(1)} \widetilde{\ell}_{i,j}^{p}(1,\xi) v^{j}(t,\xi) d\xi,$$
(53)

for  $i=1,\ldots,m$ , where  $\rho_i^p$  are given in (29) and  $\widetilde{k}_{i,l}^p,\widetilde{\ell}_{i,j}^p$  are given by (52) for all  $j=1,\ldots,m$  and  $1\leq i\leq p\leq m$ . The control law (53) exponentially stabilizes system (49), (50) on E, provided that n is sufficiently large.

# 4.3. Proof of Theorem 3

The proof of Theorem 3 is presented at the end of this section based on the following lemmas.

**Lemma 4** (Transforming n + m Kernels from E to  $E_c$ ). Consider the n + m kernel equations (C.1)–(C.5) with parameters satisfying Assumption 2 and define the following functions for all  $x \in [0, 1]$ , piecewise in y for i, l = 1, ..., n and j = 1, ..., m

$$\lambda^{n}(x, y) = \lambda_{i}(x), \quad y \in ((i-1)/n, i/n],$$
 (54a)

$$\sigma^n(x, y, \eta) = \sigma_{i,l}(x), \quad y \in ((i-1)/n, i/n],$$

$$\eta \in ((l-1)/n, l/n],$$
(54b)

$$W_i^n(x, y) = w_{i,j}(x), \quad y \in ((i-1)/n, i/n],$$
 (54c)

$$\theta_i^n(x, y) = \theta_{i,i}(x), \quad y \in ((i-1)/n, i/n],$$
 (54d)

$$Q_i^n(y) = q_{i,j}, \quad y \in ((i-1)/n, i/n].$$
 (54e)

Construct the following functions for  $(x, \xi) \in \mathcal{T}_i^p$  with  $1 \le i \le p \le m$ , piecewise in y for l = 1, ..., n

$$K_{i,p}^{n}(x,\xi,y) = k_{i,l}^{p}(x,\xi), \quad y \in (l-1)/n, l/n],$$
 (55)

where  $k_{i,l}^p$  is the solution to (C.1a) on  $\mathcal{T}_i^p$ . Then,  $K_{i,p}^n$  together with  $\ell_{i,j}^p$  for  $j=1,\ldots,m$  (the solution to (C.1b) on  $\mathcal{T}_i^p$ ) satisfy the continuum kernel equations (27), (31)–(33) with parameters defined in (54) and the original  $\mu_i, \psi_{i,j}, l_{i,j}$ , for  $i, j=1,\ldots,m$ .

**Proof.** We define the linear transform  $\mathcal{F} = \operatorname{diag}(\mathcal{F}_n, I_m)$  where  $\mathcal{F}_n \mathbf{e}_i = \chi_{((i-1)/n, i/n]}$  with  $\chi_{((i-1)/n, i/n]}$  being the indicator function of the interval ((i-1)/n, i/n] and  $(\mathbf{e}_i)_{i=1}^n$  being the Euclidean basis of  $\mathbb{R}^n$ . Thus, the transform maps any  $\mathbf{b} = (b_i)_{i=1}^{n+m} \in \mathbb{R}^{n+m}$  into  $L^2([0, 1]; \mathbb{R}) \times \mathbb{R}^m$  as

$$\mathcal{F}\mathbf{b} = \begin{bmatrix} \sum_{i=1}^{n} b_{i} \chi_{((i-1)/n, i/n]} \\ (b_{j})_{j=n+1}^{n+m} \end{bmatrix}.$$
 (56)

For any  $g \in L^2([0, 1]; \mathbb{R})$ , the adjoint  $\mathcal{F}_n^*$  satisfies

$$\langle \mathcal{F}_n \mathbf{e}_{\ell}, g \rangle_{L^2([0,1];\mathbb{R})} = \int_{(\ell-1)/n}^{\ell/n} g(y) dy = \frac{1}{n} \left\langle \mathbf{e}_{\ell}, \mathcal{F}_n^* g \right\rangle_{\mathbb{R}^n}, \tag{57}$$

that is,  $\mathcal{F}_n^*$  is given by

$$\mathcal{F}_{n}^{*}g = \left(n \int_{(i-1)/n}^{i/n} g(y) dy\right)_{i-1}^{n},$$
(58)

where each component is the mean value of g over the interval [(i-1)/n,i/n]. Thus,  $\mathcal{F}$  has the adjoint  $\mathcal{F}^*=\operatorname{diag}\left(\mathcal{F}_n^*,I_m\right)$ , which additionally satisfies  $\mathcal{F}^*\mathcal{F}=I_{n+m}$ , i.e.,  $\mathcal{F}$  (and  $\mathcal{F}_n$ ) are isometries, and thus, norm preserving from their domain to their co-domain. Now, the claim follows similarly to Humaloja and Bekiaris-Liberis (2025b, Lem. 4.2) after applying  $\mathcal{F}$  to (C.1) from the left (pointwise in  $(x,\xi)\in\mathcal{T}_i^p$  for every  $1\leq i\leq p\leq m$ ), using the fact that  $\mathcal{F}^*\mathcal{F}=I_{n+m}$  and the definitions (54), (55). Moreover, one needs to verify that the boundary conditions (31)–(33) are satisfied, which is trivially true for (31a), (32), (33a) as the  $\mathcal{F}$  transform is identity in the second component, and the remaining (31b), (31c), (33b) are verified utilizing the fact that  $K_{i,p}^n$  are piecewise constant in y.  $\square$ 

**Lemma 5** (Approximating n+m Kernels by Continuum). Consider the solutions  $K_{i,p}^n, \ell_{i,j}^p$  for  $j=1,\ldots,m, 1\leq i\leq p\leq m$  to the kernel equations (27), (31)–(33) for any  $n\in\mathbb{N}$  with parameters  $\lambda^n, \mu_j, \sigma^n, W_j^n, \theta_j^n, Q_j^n, \psi_{i,j}, l_{i,j}$ , for  $i,j=1,\ldots,m$ , from Lemma 4. There exist continuum parameters  $\lambda, \sigma, W_j, \theta_j, Q_j$  constructed such that they satisfy (51) and together with the original parameters  $\mu_j, \psi_{i,j}$  they satisfy Assumption 1. For any such parameters, the solution  $K_i^p, L_{i,j}^p$  for  $j=1,\ldots,m, 1\leq i\leq p\leq m$  to the continuum kernel equations (27), (31)–(33), where  $l_{i,j}^{(1)}=l_{i,j}$ , exists and satisfies the following implications. For any  $\delta_1>0$ , there exists an  $n_{\delta_1}\in\mathbb{N}$  such that for all  $n\geq n_{\delta_1}$  we have

$$\max_{1 \le i \le p \le m} \max_{(x,\xi) \in \mathcal{T}_i^p} \|K_i^p(x,\xi,\cdot) - K_{i,p}^n(x,\xi,\cdot)\|_{L^2} \le \delta_1, \tag{59a}$$

$$\max_{j=\{1,...,m\}} \max_{1 \le i \le p \le m} \max_{(x,\xi) \in \mathcal{T}_i^p} |L_{i,j}^p(x,\xi) - \ell_{i,j}^p(x,\xi)| \le \delta_1.$$
 (59b)

**Proof.** Following the same steps as in the proof of Humaloja and Bekiaris-Liberis (2025b, Lem. 4.3), we first note that the kernel Eqs. (27), (31)–(33) have well-posed solutions for the two sets of parameters considered in the statement of the lemma. Thus,  $K_{i,p}^n, \ell_{i,j}^p$  depend continuously on  $\lambda^n, \mu_j, \sigma^n, W_j^n, \theta_j^n, Q_j^n, \psi_{i,j}$ , and  $l_{i,j}$  by Hu et al. (2019, Thm A.1) and Lemma 4, and  $K_i^p, L_{i,j}^p$  depend continuously on  $\lambda, \mu_j, \sigma, W_j, \theta_j, Q_j, \psi_{i,j}$ , and  $l_{i,j}$  by Theorem 2, for  $i, j = 1, \ldots, m$  with  $i \leq p \leq m$ . As the parameters  $\mu_j, \psi_{i,j}, l_{i,j}$  coincide, the claim follows after showing that the parameters  $\lambda^n, \sigma^n, W_j^n, \theta_j^n, Q_j^n$  converge to  $\lambda, \sigma, W_j, \theta_j, Q_j$  (for all  $j = 1, \ldots, m$ ) as  $n \to \infty$ . This convergence is established under

<sup>&</sup>lt;sup>10</sup> If  $K_i^p(x, \xi, \cdot)$  is continuous, the mean-value sampling in (52a) can be replaced with pointwise evaluation, e.g., at  $y = 1/n, \ldots, 1$ .

(54) by Tao (2011, Sect. 1.3.5) in the sense that, for any  $\varepsilon_1 > 0$ , the following estimates are satisfied for any sufficiently large n

$$\max_{x \in [0,1]} \|\lambda(x,\cdot) - \lambda^{n}(x,\cdot)\|_{L^{2}([0,1];\mathbb{R})} \le \varepsilon_{1}, \tag{60a}$$

$$\max_{\mathbf{x} \in [0,1]} \|\sigma(\mathbf{x}, \cdot) - \sigma^{n}(\mathbf{x}, \cdot)\|_{L^{2}([0,1]^{2}; \mathbb{R})} \le \varepsilon_{1}, \tag{60b}$$

$$\max_{j=1,\dots,m} \max_{x \in [0,1]} \|\theta_j(x,\cdot) - \theta_j^n(x,\cdot)\|_{L^2([0,1];\mathbb{R})} \le \varepsilon_1, \tag{60c}$$

$$\max_{j=1,\dots,m} \max_{x \in [0,1]} \|W_j(x,\cdot) - W_j^n(x,\cdot)\|_{L^2([0,1];\mathbb{R})} \le \varepsilon_1, \tag{60d}$$

$$\max_{j=1,...,m} \|Q_j - Q_j^n\|_{L^2([0,1];\mathbb{R})} \le \varepsilon_1. \quad \Box$$
 (60e)

**Remark 3.** As noted in Humaloja and Bekiaris-Liberis (2025b, Rem. 4.4), the step functions  $\lambda^n$ ,  $\sigma^n$ ,  $\theta^n_j$ ,  $W^n_j$ ,  $Q^n_j$  could be constructed in various, alternative ways to (54), but the result of Lemma 5 remains valid as long as the step functions approximate the continuous functions  $\lambda$ ,  $\sigma$ ,  $\theta_j$ ,  $W_j$ ,  $Q_j$  (satisfying (51)) to arbitrary accuracy as  $n \to \infty$  as in (60).

**Lemma 6** (Representation of (53) as Perturbation of Exact Controller). The control law (53) can be written as

$$\begin{split} U^{i}(t) &= \sum_{l=1}^{n} \sum_{p=i}^{m} \int_{\rho_{i}^{p+1}(1)}^{\rho_{i}^{p}(1)} \frac{1}{n} k_{i,l}^{p}(1,\xi) u^{l}(t,\xi) d\xi \\ &+ \sum_{j=1}^{m} \sum_{p=i}^{m} \int_{\rho_{i}^{p+1}(1)}^{\rho_{i}^{p}(1)} \ell_{i,j}^{p}(1,\xi) v^{j}(t,\xi) d\xi \\ &+ \sum_{l=1}^{n} \sum_{i=1}^{m} \int_{\rho_{i}^{p+1}(1)}^{\rho_{i}^{p}(1)} \frac{1}{n} \Delta k_{i,l}^{p}(1,\xi) u^{l}(t,\xi) d\xi \end{split}$$

 $+\sum_{i=1}^{m}\sum_{j=1}^{m}\int_{\rho_{i}^{p+1}(1)}^{\rho_{i}^{p}(1)}\Delta\ell_{i,j}^{p}(1,\xi)v^{j}(t,\xi)d\xi,$ 

where  $k_{i,l}^p$ ,  $\ell_{i,j}^p$  is the (exact) solution to the n+m kernel equations (C.1)–(C.5) and  $\Delta k_{i,l}^p$ ,  $\Delta \ell_{i,j}^p$  are the approximation error terms that become arbitrarily small, uniformly in  $\xi \in [\rho_i^{p+1}(1), \rho_i^p(1)]$ , for all  $l=1,\ldots,n$  and  $i,j=1,\ldots,m$  with  $i \leq p \leq m$ , when n is sufficiently large.

**Proof.** Transform the functions  $\widetilde{k}_{i,l}^p$  from (52) into step functions in v as

$$\widetilde{K}_{i,n}^{n}(x,\xi,y) = \widetilde{k}_{i,l}^{p}(x,\xi), \quad y \in ((l-1)/n,l/n],$$
(62)

for all  $(x,\xi)\in\mathcal{T}_i^p$  and  $1\leq i\leq p\leq m$ , piecewise for y for  $l=1,2,\ldots,n$ . By (52) and (62), we have  $\widetilde{K}_{i,p}^n(x,\xi,\cdot)=\mathcal{F}_n\mathcal{F}_n^*K_i^p(x,\xi,\cdot)$ , which is the mean-value approximation of  $K_i^p(x,\xi,\cdot)$  for all  $(x,\xi)\in\mathcal{T}_i^p$  and  $1\leq i\leq p\leq m$ . By Tao (2011, Sect. 1.6), the mean-value approximation becomes arbitrarily accurate for sufficiently large n, i.e., for any  $\varepsilon_2>0$  there exists some  $n_{\varepsilon_2}\in\mathbb{N}$  such that

$$\max_{1 \le i \le p \le m} \max_{(x,\xi) \in \mathcal{T}_i^p} \|K_i^p(x,\xi,\cdot) - \widetilde{K}_{i,p}^n(x,\xi,\cdot)\|_{L^2} \le \varepsilon_2, \tag{63}$$

for any  $n \ge n_{\varepsilon_2}$ . Combining (63) with the estimate (59a) and using the triangle inequality, we have for any  $n \ge \max\{n_{\delta_1}, n_{\varepsilon_2}\}$ 

$$\begin{split} \max_{1\leq i\leq p\leq m} \max_{(x,\xi)\in\mathcal{T}_{i}^{p}} \|K_{i,p}^{n}(x,\xi,\cdot) - \widetilde{K}_{i,p}^{n}(x,\xi,\cdot)\|_{L^{2}} \leq \\ \max_{1\leq i\leq p\leq m} \max_{(x,\xi)\in\mathcal{T}_{i}^{p}} \|K_{i}^{p}(x,\xi,\cdot) - K_{i,p}^{n}(x,\xi,\cdot)\|_{L^{2}} \\ + \max_{1\leq i\leq p\leq m} \max_{(x,\xi)\in\mathcal{T}_{i}^{p}} \|K_{i}^{p}(x,\xi,\cdot) - \widetilde{K}_{i,p}^{n}(x,\xi,\cdot)\|_{L^{2}} \leq \end{split}$$

$$\delta_1 + \varepsilon_2$$
, (64)

where both  $\delta_1$  and  $\varepsilon_2$  can be made arbitrarily small by increasing n, which follows from Lemma 5 and (62), respectively. As the estimate is uniform on every  $\mathcal{T}_i^p$ , it particularly applies on x = 1.

Moreover, the step functions  $\widetilde{K}_{i,p}^n$  and  $K_{i,p}^n$  constructed in (55) and (62), respectively, are obtained through applying the transform  $\mathcal{F}_n$ , introduced in the proof of Lemma 4, to  $(\widetilde{k}_{i,l}^p)_{l=1}^n$  and  $(k_{i,l}^p)_{l=1}^n$ , respectively, for all  $i=1,\ldots,m$ . Thus, as  $\mathcal{F}_n$  is an isometry, the estimate (64) also holds for these functions, i.e.,

$$\max_{1 \leq i \leq p \leq m} \max_{(x,\xi) \in \mathcal{T}_{i}^{p}} \frac{1}{\sqrt{n}} \left\| \left( k_{i,l}^{p}(x,\xi) \right)_{l=1}^{n} - \left( \widetilde{k}_{i,l}^{p}(x,\xi) \right)_{l=1}^{n} \right\|_{\mathbb{R}^{n}} \leq \delta_{1} + \varepsilon_{2}. \tag{65}$$

In addition, from (59b) in Lemma 5 we already have for  $n \ge n_{\delta_1}$ 

$$\max_{1 \le i \le p \le m} \max_{(x,\xi) \in \mathcal{T}_i^p} \left\| \left( \ell_{i,j}^p(x,\xi) \right)_{j=1}^m - \left( \widetilde{\ell}_{i,j}^p(x,\xi) \right)_{j=1}^m \right\|_{\mathbb{R}^m} \le \sqrt{m} \delta_1.$$
(66)

Now, setting  $\Delta k_{i,l}^p = \widetilde{k}_{i,l}^p - k_{i,l}^p$  and  $\Delta \ell_{i,j}^p = \widetilde{\ell}_{i,j}^p - \ell_{i,j}^p$ , we have written (53) as (61), where the error term can be estimated using (65), (66), triangle inequality, and Cauchy–Schwarz inequality, for all  $i = 1, \ldots, m$ , as

$$\sum_{l=1}^{n} \sum_{p=i}^{m} \int_{\rho_{i}^{p+1}(1)}^{\rho_{i}^{p}(1)} \frac{1}{n} \Delta k_{i,l}^{p}(1,\xi) u^{l}(t,\xi) d\xi 
+ \sum_{j=1}^{m} \sum_{p=i}^{m} \int_{\rho_{i}^{p+1}(1)}^{\rho_{i}^{p}(1)} \Delta \ell_{i,j}^{p}(1,\xi) v^{j}(t,\xi) d\xi \le 
(\delta_{1} + \varepsilon_{2} + \sqrt{m}\delta_{1}) \left\| \left( \frac{\mathbf{u}(t,\cdot)}{\mathbf{v}(t,\cdot)} \right) \right\|_{F},$$
(67)

where  $\delta_1$  and  $\varepsilon_2$  become arbitrarily small when n is sufficiently large.  $\square$ 

*Proof of Theorem* 3. By Lemma 6, the control law (53) splits into two parts as shown in (61), where the first part exponentially stabilizes the system (49), (50) by Hu et al. (2019, Thm 2.1), while the second one becomes arbitrarily small when n is arbitrarily large. Thus, the exponential stability of the closed-loop system (49), (50) under control law (61), when n is sufficiently large, follows directly from the well-posedness of (49), (50) (see Remark 2) and Humaloja and Bekiaris-Liberis (2025b, Prop. A.2).

**Remark 4.** In order to quantify an upper bound on  $\delta_1$  and  $\varepsilon_2$  in (67), one can employ Lyapunov-based arguments similarly to Humaloja and Bekiaris-Liberis (2025b, App. C.4). A Lyapunov functional for (49), (50) under the control law (61) can be constructed similarly to (18) for  $\mathbf{u}(t,\cdot) \in L^2([0,1];\mathbb{R}^n)$  (see also Hu et al. (2019, Prop. 2.1)), i.e.,

$$\widetilde{V}(t) = \int_0^1 \left( e^{-\widetilde{\delta}x} \| \mathbf{u}(t, x) \|_{\mathbf{\Lambda}^{-1}}^2 + e^{\widetilde{\delta}x} \| \boldsymbol{\beta}(t, x) \|_{\widetilde{\mathbf{D}}\mathbf{M}^{-1}}^2 \right) dx, \tag{68}$$

where  $\boldsymbol{\beta}$  is defined for  $\mathbf{u}(t,\cdot) \in L^2([0,1];\mathbb{R}^n)$  in Hu et al. (2016, (28)) and satisfies (8b), (9b). The stability analysis follows the same steps as in the proof of Theorem 1, which results in

$$\dot{\widetilde{V}}(t) \le -\frac{\widetilde{c}_V}{\max\left\{\widetilde{M}_{\mu}, \widetilde{M}_{\lambda}\right\}} \widetilde{V}(t) + e^{\widetilde{\delta}x} \|\boldsymbol{\beta}(1, t)\|_{\widetilde{\mathbf{p}}}^2, \tag{69}$$

for some  $\tilde{c}_V$ ,  $\widetilde{M}_{\mu}$ ,  $\widetilde{M}_{\lambda} > 0$ , where the boundary condition in  $\boldsymbol{\beta}(t, 1)$  is not zero but it is given by the error terms in the control law (61). Given the estimate (67) and since by Hu et al. (2016, Thm.

(61)

3.4) the n+m backstepping transformation (of  $\beta$ ) is invertible, we can estimate from (61)

$$\|\boldsymbol{\beta}(t,1)\|_{\widetilde{\mathbf{D}}}^2 \le \|\widetilde{\mathbf{D}}\|_{\infty} m^2 (\delta_1 + \varepsilon_2 + \sqrt{m}\delta_1)^2 M_V^2 \left\| \begin{pmatrix} \mathbf{u}^{(t,\cdot)} \\ \boldsymbol{\beta}^{(t,\cdot)} \end{pmatrix} \right\|_{r}^2, \tag{70}$$

where  $M_V$  is a bound on the inverse backstepping transformation of  $\boldsymbol{\beta}$  for the n+m case (see Hu et al. (2016, (45))). Now, if  $\tilde{\delta}$ ,  $\tilde{\mathbf{D}} > 0$  have been fixed such that (69) holds for  $\boldsymbol{\beta}(1,t) = 0$ , for  $\delta_1, \varepsilon_2 > 0$  sufficiently small, given a sufficiently large n,  $\tilde{V}$  remains negative definite also when  $\boldsymbol{\beta}(1,t)$  is estimated with (70).

# 5. Convergence of the large-scale system to a continuum

While in Section 4 we present an approximation result that concerns backstepping kernels, in the present section we provide a formal proof that the actual solutions of the PDE system (49), (50) converge to the solutions of the continuum PDE system (4), (5), as  $n \to \infty$ . The following result is of interest itself as it provides a formal connection between the solutions of the n+m system and the solutions of its continuum counterpart.

**Theorem 4.** Consider an n+m system (49), (50) with parameters  $\mu_j, \psi_{j,\ell}, \theta_{j,i}, w_{i,j}, q_{i,j}, \lambda_i$ , and  $\sigma_{i,l}$  for  $i,l=1,\ldots,n$  and  $j,\ell=1,\ldots,m$ , satisfying Assumption 2, initial conditions  $(\mathbf{u}_0,\mathbf{v}_0)\in E$ , and input  $\mathbf{U}\in L^2_{loc}([0,+\infty);\mathbb{R}^m)$ . Construct a continuum system (4), (5) with parameters  $\lambda,\mu_j,\sigma,\theta_j,W_j,Q_j,\psi_{j,\ell}$  for  $j,\ell=1,\ldots,m$  that satisfy Assumption 1 and (51), and equip (4), (5) with initial conditions  $u_0,\mathbf{v}_0$  and input  $\mathbf{U}$ , such that  $u_0$  is continuous in y and satisfies

$$u_0(x, i/n) = u_0^i(x), \quad i = 1, \dots, n.$$
 (71)

Sample the solution  $(u, \mathbf{v})$  to the resulting PDE system (4), (5) for these data into a vector-valued function  $(\widetilde{\mathbf{u}}, \widetilde{\mathbf{v}})$  as  $\widetilde{\mathbf{u}}(t, x) = \mathcal{F}_n^* u(t, x, \cdot)$  (see (58)) and  $\widetilde{\mathbf{v}}(t, x) = \mathbf{v}(t, x)$ , pointwise for all  $t \geq 0$  and almost all  $x \in [0, 1]$ . On any compact interval  $t \in [0, T]$ , for any given T > 0, we have

$$\max_{t \in [0,T]} \left\| \begin{pmatrix} \mathbf{u}(t) \\ \mathbf{v}(t) \end{pmatrix} - \begin{pmatrix} \widetilde{\mathbf{u}}(t) \\ \widetilde{\mathbf{v}}(t) \end{pmatrix} \right\|_{E} \le \varepsilon_{3}, \tag{72}$$

where  $\varepsilon_3 > 0$  becomes arbitrarily small when n is sufficiently large.

**Proof.** The statement follows applying the same steps as in the proof of Humaloja and Bekiaris-Liberis (2025b, Thm 6.1). In a nutshell, as the systems (49), (4) and (50), (5) have well-posed solutions under the assumptions of the theorem by Remark 2 and Remark 1, respectively, the solutions in particular depend continuously on the parameters, initial conditions, and inputs of the respective PDEs. Now, as the input to (49), (4) and (50), (5) is the same, while the respective parameters converge as in (60) and  $u_0$  can be approximated to arbitrary accuracy by  $\mathcal{F}_n \mathbf{u}_0$  due to (71), we have that  $\mathcal{F}\begin{pmatrix}\mathbf{u}_n^{(t)}\\\mathbf{v}_n^{(t)}\end{pmatrix}$  approximates  $\begin{pmatrix}\mathbf{u}_n^{(t)}\\\mathbf{v}_n^{(t)}\end{pmatrix}$  arbitrary accuracy on  $E_c$ , when n is sufficiently large. Since  $\mathbf{u}(t,x) = \mathcal{F}_n^* u(t,x,\cdot)$  and  $\widetilde{\mathbf{v}}(t,x) = \mathbf{v}(t,x)$ , while  $\mathcal{F}_n$  (and  $\mathcal{F}$ ) is an isometry and the mean-value approximation  $\mathcal{F}_n\mathcal{F}_n^* u(t)$  of the solution u(t) (which is bounded on  $t \in [0,T]$ ) is convergent (in  $L^2$ ; see Tao (2011, Sect. 1.6)), the estimate (72) follows by the triangle inequality as in Humaloja and Bekiaris-Liberis (2025b, (C.43)).

#### 6. Numerical example and simulation results

Consider the parameters for  $x, y, \eta \in [0, 1]$ 

$$\lambda(x, y) = 1, \quad \mu_1(x) = 2, \quad \mu_2(x) = 1,$$
 (73a)

$$\sigma(x, y, \eta) = x^3(x+1)\left(y - \frac{1}{2}\right)\left(\eta - \frac{1}{2}\right),$$
 (73b)

$$W_1(x, y) = W_2(x, y) = x(x+1)e^x \left(y - \frac{1}{2}\right),$$
 (73c)

$$\theta_1(x, y) = -3y(y - 1), \quad \theta_2(x, y) = -2y(y - 1),$$
 (73d)

$$\psi_{i,j}(x) = 0, \quad i, j \in \{1, 2\},$$
 (73e)

$$Q_1(y) = 8\left(y - \frac{1}{2}\right), \quad Q_2(y) = -8(y - 2),$$
 (73f)

corresponding to an  $\infty + m$  system for m = 2, which can be viewed as a continuum approximation of an n + m system (for large n) based on (51) with respective parameters

$$\lambda_i(x) = 1, \tag{74a}$$

$$\sigma_{i,l}(x) = x^3(x+1)\left(\frac{i}{n} - \frac{1}{2}\right)\left(\frac{l}{n} - \frac{1}{2}\right),$$
 (74b)

$$\theta_{1,i}(x) = -3\frac{i}{n}\left(\frac{i}{n} - 1\right), \quad \theta_{2,i}(x) = -2\frac{i}{n}\left(\frac{i}{n} - 1\right),$$
 (74c)

$$w_{i,1}(x) = w_{i,2}(x) = x(x+1)e^{x}\left(\frac{i}{n} - \frac{1}{2}\right),$$
 (74d)

$$q_{i,1} = 8\left(\frac{i}{n} - \frac{1}{2}\right), \quad q_{i,2} = -8\left(\frac{i}{n} - 2\right),$$
 (74e)

for  $i, l=1,\ldots,n$ . For the parameters (73), the solution to the continuum kernel equations (27), (31)–(33), where we choose  $l_{2,1}^{(1)}=\psi_{2,1}=0$ , is explicitly given by

$$K_1^1(x, \xi, y) = y(y - 1),$$
 (75a)

$$K_1^2(x,\xi,y) = e^{x-2\xi}y(y-1),$$
 (75b)

$$K_2^2(x, \xi, y) = e^{2(x-\xi)}y(y-1),$$
 (75c)

$$L_{1,1}^1(x,\xi) = L_{1,1}^2(x,\xi) = 0,$$
 (75d)

$$L_{1,2}^{1}(x,\xi) = 0, \quad L_{1,2}^{2}(x,\xi) = -2e^{x-2\xi},$$
 (75e)

$$L_{2,1}^2(x,\xi) = 0, \quad L_{2,2}^2(x,\xi) = -2e^{2(x-\xi)},$$
 (75f)

where  $K_1^{\star}(\cdot,y)$ ,  $L_{1,1}^{\star}$ , and  $L_{1,2}^{\star}$  are defined on  $\mathcal{T}_1^1=\{(x,\xi)\in[0,1]^2:\frac{1}{2}x\leq\xi\leq x\}$  and  $\mathcal{T}_1^2=\{(x,\xi)\in[0,1]^2:\xi\leq\frac{1}{2}x\}$  for the respective superindex  $\star=1,2$ , while  $K_2^2(\cdot,y),L_{2,1}^2$  and  $L_{2,2}^2$  are defined on  $\mathcal{T}_2^2=\mathcal{T}$ , for each  $y\in[0,1]$ . Note the discontinuity in  $L_{1,2}$  along  $\xi=\frac{1}{2}x$ . In case the explicit solution is not available, one could employ, e.g., the methods of characteristics and successive approximations, as in Section 3, or a power series-based approach (as in Humaloja and Bekiaris-Liberis (2025a)) to numerically evaluate the solution.

We implement the control law (53) with (52) for n+m systems with parameters (74) for n=2,6,10 (and the same  $\mu,\Psi$  as in (73)). As the continuum kernels (75) are continuous in y, we approximate the exact n+m kernels by sampling pointwise  $K_1^1,K_1^2$ , and  $K_2^2$  at  $y=1/n,2/n,\ldots,1$  instead of using (52a) (see Footnote 10).

For the simulation, the n+m system (49), (50) is approximated by finite differences with 256 grid points in  $x \in [0, 1]$ . The ODE resulting from the finite-difference approximation is solved using ode45 in MATLAB. The initial conditions are  $u_0^i(x) = q_{i,1} + q_{i,2}$ , for  $i=1,\ldots,n$ , and  $v_0^1(x) = v_0^2(x) = 1$ , for all  $x \in [0,1]$ . The simulation results for  $t \in [0,5]$  are shown in Figs. 2 and 3, which show the controls (53) for n=2,6,10 along with the exact controls for n=10 (computed using the kernels in Appendix C) and the solution components  $u^n$  and  $v^1$  for n=10, respectively. We note that the controls shown in Fig. 2 act as weighted averages of the solution components, but since  $K_1^1, K_1^2$ , and  $K_2^2$  vanish at y=1 and  $L_{1,1}=L_{2,1}=0$ , the solution components  $u^n$  and  $v^1$  do not affect the control law and are hence displayed separately in Fig. 3 for n=10.

Based on Figs. 2 and 3, we conclude that the control law (53) based on the continuum kernels (75) exponentially stabilizes the

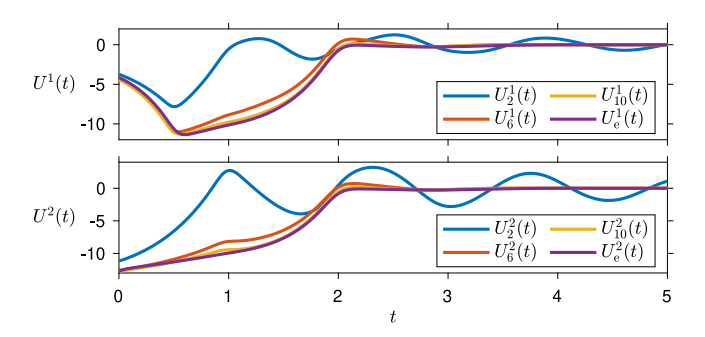


**Fig. 2.** The controls U(t) based on the approximate control law (53) for n = 2, 6, 10 and the respective exact control law for n = 10.

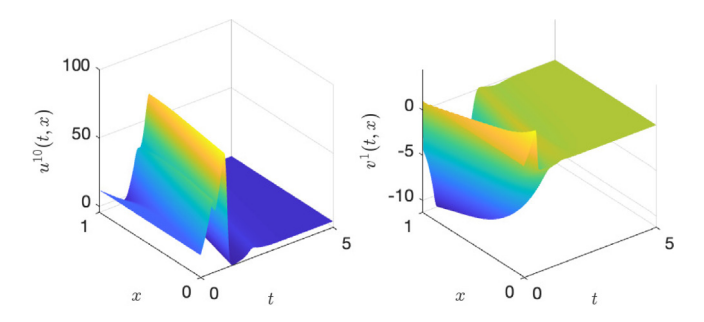


**Fig. 3.** The solution components  $u^n(t, x)$  and  $v^1(t, x)$  for n = 10.

n+m system for n=2,6,10 (and m=2), <sup>11</sup> with improved performance for larger n. This verifies the theoretical results. Furthermore, based on Fig. 2, the continuum kernels-based control law tends close to the exact control law computed based on the n+m kernels, as n increases. We note that the n+m kernels are computed based on a finite-difference approximation of the n+m kernel equations in Appendix C, since we were not able to find the solution in closed form.

# 7. Conclusions and discussion

We introduced a backstepping control design methodology for a class of continua of hyperbolic PDE systems. Well-posedness of the derived kernel equations was established, together with exponential stability of the closed-loop system. We then utilize the continuum backstepping kernels for stabilization of a largescale system counterpart, establishing that, as  $n \rightarrow \infty$ , the continuum kernels can approximate (to arbitrary accuracy) the exact backstepping kernels (constructed via applying backstepping to the large-scale system). This allowed us to prove that the control design constructed on the basis of the continuum PDE system can stabilize the respective large-scale system, which may be particularly useful, as, with this approach, complexity of computation of stabilizing kernels may not grow with the number n of PDE systems components. This was also demonstrated in a numerical example for which the continuum kernels were obtained in closed form, but for which the respective, large-scale kernels did not exhibit a closed-form solution. We also provided a formal convergence result of the solutions of the large-scale PDE system to the solutions of the respective continuum.

The case  $m \to \infty$  requires a quite different treatment through development of new analysis tools that cannot be obtained in an obvious manner via extending the tools developed here. Some

of the main reasons for this are the following. As  $m \to \infty$  the input space changes from  $\mathbb{R}^m$  to, e.g.,  $L^2([0, 1]; \mathbb{R})$ , which may impose important changes in the present analysis and results. In particular, as the exact, control inputs themselves (rather than the respective control kernels) would have to be approximated (in a certain sense), it is neither clear what are the stability properties of the closed-loop system one would obtain nor how to translate the analysis performed for finite m to the case  $m \to \infty$ . In fact, in contrast to the present paper that deals with approximation of the control kernels, which gives rise to a bounded, vanishing perturbation that preserves exponential stability, in the case of control inputs approximation one may have to prove a type of practical stability with a residual value that tends to zero as  $m \to \infty$ , which would require introduction of a different, stability proof strategy (in particular, a respective result to Theorem 4 of solutions' convergence may be essential). Furthermore, the characteristic curves would become 3-D regions, which makes the respective well-posedness analysis of the kernels much more involved. In particular, it is not obvious how one would then have to split the 4-D domain of evolution of the kernels into subdomains in which the kernels are continuous, which involves deriving 3-D discontinuity regions. In addition, the case  $m \rightarrow$  $\infty$  may impose important challenges in the purely technical steps. In particular, as the transport speeds  $\mu_i$  would become a function of two variables, namely  $\mu(x, \eta)$ , it is not obvious how the assumptions made here (e.g., (7)) would have to be translated. In turn, this imposes challenges on how the wellposedness analysis of the kernels would have to be carried out, as, for example, one may have to properly translate the boundary conditions (e.g., (31a)), as well as to re-derive from scratch certain bounds (e.g., corresponding to (44a), (46)), specifically for the case  $m \to \infty$ .

#### Acknowledgment

Funded by the European Union (ERC, C-NORA, 101088147). Views and opinions expressed are however those of the authors only and do not necessarily reflect those of the European Union or the European Research Council Executive Agency. Neither the European Union nor the granting authority can be held responsible for them.

## Appendix A. Derivation of continuum kernel equations (12)

Let us first differentiate (11b) with respect to x and use the Leibniz rule to get

$$\boldsymbol{\beta}_{x}(t,x) = \mathbf{v}_{x}(t,x) - \mathbf{L}(x,x)\mathbf{v}(t,x) - \int_{0}^{1} \mathbf{K}(x,x,y)u(t,x,y)dy$$
$$-\int_{0}^{x} \mathbf{L}_{x}(x,\xi)\mathbf{v}(t,\xi)d\xi - \int_{0}^{x} \int_{0}^{1} \mathbf{K}_{x}(x,\xi,y)u(t,\xi,y)dyd\xi.$$
(A.1)

Moreover, differentiating (11b) with respect to t and using (4b) gives

$$\boldsymbol{\beta}_{t}(t,x) = \mathbf{M}(x)\mathbf{v}_{x}(t,x) + \int_{0}^{1} \Theta(x,y)u(t,x,y)dy$$

$$+ \Psi(x)\mathbf{v}(t,x) - \int_{0}^{x} \mathbf{L}(x,\xi)\mathbf{M}(\xi)\mathbf{v}_{\xi}(t,\xi)d\xi$$

$$- \int_{0}^{x} \mathbf{L}(x,\xi) \int_{0}^{1} \Theta(\xi,y)u(t,\xi,y)dyd\xi$$

$$- \int_{0}^{x} \mathbf{L}(x,\xi)\Psi(\xi)\mathbf{v}(t,\xi)d\xi$$

<sup>&</sup>lt;sup>11</sup> Based on numerical simulations, the n+2 system with parameters (74) is unstable for any  $n \ge 2$ .

and

$$+ \int_{0}^{x} \int_{0}^{1} \mathbf{K}(x, \xi, y) \lambda(\xi, y) u_{\xi}(t, \xi, y) dy d\xi$$

$$- \int_{0}^{x} \int_{0}^{1} \mathbf{K}(x, \xi, y) \int_{0}^{1} \sigma(\xi, y, \eta) u(t, \xi, \eta) d\eta dy d\xi$$

$$- \int_{0}^{x} \int_{0}^{1} \mathbf{K}(x, \xi, y) \mathbf{W}(\xi, y) \mathbf{v}(t, \xi) dy d\xi, \tag{A.2}$$

where integration by parts further gives

$$\int_{0}^{x} \mathbf{L}(x,\xi) \mathbf{M}(\xi) \mathbf{v}_{\xi}(t,\xi) d\xi =$$

$$\mathbf{L}(x,x) \mathbf{M}(x) \mathbf{v}(t,x) - \mathbf{L}(x,0) \mathbf{M}(0) \mathbf{v}(t,0)$$

$$-\int_{0}^{x} \left( \mathbf{L}_{\xi}(x,\xi) \mathbf{M}(\xi) + \mathbf{L}(x,\xi) \mathbf{M}'(\xi) \right) \mathbf{v}(t,\xi) d\xi, \tag{A.3}$$

 $\int_{0}^{x} \mathbf{K}(x, \xi, y) \lambda(\xi, y) u_{\xi}(t, \xi, y) d\xi =$   $\mathbf{K}(x, x, y) \lambda(x, y) u(t, x, y) - \mathbf{K}(x, 0, y) \lambda(0, y) u(t, 0, y)$   $- \int_{0}^{x} (\mathbf{K}_{\xi}(x, \xi, y) \lambda(\xi, y) + \mathbf{K}(x, \xi, y) \lambda_{\xi}(\xi, y)) u(t, \xi, y) d\xi. \tag{A.4}$ 

Thus, in order for (8) to hold, the kernels **L** and **K** need to satisfy (12), (13), where we also used (9a) with  $\alpha(t, 0, \cdot) = u(t, 0, \cdot)$  and  $\boldsymbol{\beta}(t, 0) = \mathbf{v}(t, 0)$  for all  $t \geq 0$ . Moreover, inserting (11) into (8a) gives that  $\mathbf{C}^-$  and  $C^+$  need to satisfy

$$\mathbf{C}^{-}(x,\xi,y) = \mathbf{W}(x,y)\mathbf{L}(x,\xi) + \int_{\xi}^{x} \mathbf{C}^{-}(x,\zeta,y)\mathbf{L}(\zeta,\xi)d\zeta, \quad (A.5a)$$

$$C^{+}(x,\xi,y,\eta) = \mathbf{W}(x,y)\mathbf{K}(x,\xi,\eta)$$

$$+ \int_{\xi}^{x} \mathbf{C}^{-}(x,\zeta,y)\mathbf{K}(\zeta,\xi,\eta)d\zeta, \quad (A.5b)$$

for almost all  $0 \le \xi \le x \le 1$  and  $y, \eta \in [0, 1]$  (when applicable). Once **L** and **K** are solved from the kernel Eqs. (12), (13), then (A.5a) is a Volterra equation of second kind, and well-studied in the literature. We show in Lemma 7 that (A.5a) has a well-posed solution  $\mathbf{C}^- \in L^\infty(\mathcal{T}; L^2([0, 1]; \mathbb{R}^{1 \times m}))$ . Once  $\mathbf{C}^-$  is solved from (A.5a),  $C^+$  is explicitly given as a function of **W**, **K** and  $\mathbf{C}^-$  by (A.5b), by which  $C^+ \in L^\infty(\mathcal{T}; L^2([0, 1]^2; \mathbb{R}))$  follows.

**Lemma 7.** Under Assumption 1, Eq. (A.5a) admits a unique solution  $\mathbf{C}^- \in L^\infty(\mathcal{T}; L^2([0, 1]; \mathbb{R}^{1 \times m}))$ .

**Proof.** Utilizing similar tools as in Hochstadt (1989, Thm 2.3.5) and Hu et al. (2019, Thm. A.2), we show that  $C^-$  is given by the series

$$\mathbf{C}^{-}(x,\xi,y) = \sum_{k=0}^{\infty} \Delta \mathbf{C}_{k}^{-}(x,\xi,y), \tag{A.6}$$

where  $\Delta \mathbf{C}_0^-(x,\xi,y) = \mathbf{W}(x,y)\mathbf{L}(x,\xi)$ , so that  $\Delta \mathbf{C}_0 \in C(\mathcal{T}_i^p; L^2([0,1];\mathbb{R}))$  for any  $1 \leq i \leq p \leq m$  by Theorem 2, and  $\Delta \mathbf{C}_k^-$  for  $k \geq 1$  is defined recursively by

$$\Delta \mathbf{C}_{k}^{-}(x,\xi,y) = \int_{\xi}^{x} \Delta \mathbf{C}_{k-1}^{-}(x,\zeta,y) \mathbf{L}(\zeta,\xi) d\zeta, \tag{A.7}$$

by which  $\Delta \mathbf{C}_k^- \in C(\mathcal{T}_i^p; L^2([0, 1]; \mathbb{R}))$  for  $k \geq 1$ . By induction, it immediately follows that  $\Delta \mathbf{C}_k$  satisfy

$$\max_{j \in \{1, ..., m\}} \operatorname{esssup}_{(x, \xi) \in \mathcal{T}} \| \left( \Delta C_j^- \right)_k (x, \xi, \cdot) \|_{L^2} \le M_W \frac{(M_L)^{k+1} (x - \xi)^k}{k!}, \tag{A.8}$$

where

$$M_{L} = \max_{i,j \in \{1,\dots,m\}} \underset{(x,\xi) \in \mathcal{T}}{\operatorname{esssup}} \left| L_{i,j}(x,\xi) \right|, \tag{A.9}$$

and  $M_W$  is given in (20d). Thus, the series (A.6) converges on  $L^{\infty}(\mathcal{T}; L^2([0, 1]; \mathbb{R}))$  to the stated solution to (A.5a).  $\square$ 

#### Appendix B. Invertibility of (11)

**Lemma 8.** *Under Assumption* 1, the transformation (11) is boundedly invertible on  $E_c$ .

**Proof.** The claim follows after solving for  $(u, \mathbf{v})$  from (11). Since  $u = \alpha$ , inserting this to (11b) gives

$$\mathbf{v}(t,x) - \int_0^x \mathbf{L}(x,\xi)\mathbf{v}(t,\xi)d\xi =$$

$$\int_0^x \int_0^1 \mathbf{K}(x,\xi,y)\alpha(t,\xi,y)dyd\xi - \boldsymbol{\beta}(t,x), \tag{B.1}$$

which is a Volterra equation of second kind for  $\mathbf{v}(t,\cdot)$  in terms of  $\alpha(t,\cdot)$ ,  $\boldsymbol{\beta}(t,\cdot)$ ,  $\mathbf{L}$ , and  $\mathbf{K}$ , for any (fixed)  $t \geq 0$ . Since  $(\alpha,\boldsymbol{\beta}) \in C([0,+\infty);E_c)$ , being the solution to (8), (9) (by Theorem 1), and as  $\mathbf{K} \in L^{\infty}(\mathcal{T};L^2([0,1];\mathbb{R}^m))$ ,  $\mathbf{L} \in L^{\infty}(\mathcal{T};\mathbb{R}^{m \times m})$  by Theorem 2, Eq. (B.1) has a unique solution  $\mathbf{v}(t,\cdot) \in L^2([0,1];\mathbb{R}^m)$  for all  $t \geq 0$  by Hochstadt (1989, Thm 2.3.6).  $\square$ 

# Appendix C. Kernel equations for linear hyperbolic n+m PDEs

Denote  $\mathbf{k}_{i}^{p} = \left(k_{i,l}^{p}\right)_{l=1}^{n}$  and  $\boldsymbol{\ell}_{i}^{p} = \left(\ell_{i,j}^{p}\right)_{j=1}^{m}$ , where  $k_{i,l}^{p}, \ell_{i,j}^{p}$  for  $l=1,\ldots,n, j=1,\ldots,m$ , and  $1 \leq i \leq p \leq m$  denote the n+m kernels restricted to  $\mathcal{T}_{i}^{p}$ . Using the notation of (49), (50), these satisfy the kernel equations (cf. Hu et al. (2019, (A.19)–(A.23)))

$$\mu_i(x)\partial_x \mathbf{k}_i^p(x,\xi) - \mathbf{\Lambda}(\xi)\partial_\xi \mathbf{k}_i^p(x,\xi) - \mathbf{\Lambda}'(\xi)\mathbf{k}_i^p(x,\xi) =$$

$$\frac{1}{n} \mathbf{\Sigma}^{T}(\xi) \mathbf{k}_{i}^{p}(x,\xi) + \mathbf{\Theta}^{T}(\xi) \boldsymbol{\ell}_{i}^{p}(x,\xi), \tag{C.1a}$$

 $\mu_i(x)\partial_x \boldsymbol{\ell}_i^p(x,\xi) + \mathbf{M}(\xi)\partial_{\xi} \boldsymbol{\ell}_i^p(x,\xi) + \mathbf{M}'(\xi)\boldsymbol{\ell}_i^p(x,\xi) =$ 

$$\frac{1}{n}\mathbf{W}^{T}(\xi)\mathbf{k}_{i}^{p}(x,\xi) + \mathbf{\Psi}^{T}(\xi)\boldsymbol{\ell}_{i}^{p}(x,\xi), \tag{C.1b}$$

on  $\mathcal{T}_i^p$ ,  $1 \le i \le p \le m$ , with boundary conditions

$$\mu_i(x)\mathbf{k}_i^i(x,x) + \Lambda(x)\mathbf{k}_i^i(x,x) = -\Theta_{i}^T(x), \tag{C.2a}$$

$$\mu_i(x)\boldsymbol{\ell}_i^i(x,x) - \mathbf{M}(x)\boldsymbol{\ell}_i^i(x,x) = -\boldsymbol{\Psi}_{i,\cdot}^T(x), \tag{C.2b}$$

$$\frac{1}{n}\mathbf{Q}^{T}\mathbf{\Lambda}(0)\mathbf{k}_{i}^{m}(x,0) - \mathbf{M}(0)\boldsymbol{\ell}_{i}^{m}(x,0) = \mathbf{g}_{i}(x), \tag{C.2c}$$

where  $\mathbf{g}_i = \left(g_{i,j}\right)_{j=1}^m$  satisfies  $g_{i,j} = 0$  for  $i \leq j$ . Additionally, an artificial boundary condition is imposed to guarantee well-posedness of the kernel equations as follows

$$\forall j < i: \ \ell_{i,j}^p(1,\xi) = l_{i,j}(\xi),$$
 (C.3)

where the functions  $l_{i,j}$  can be chosen arbitrarily. However, we choose  $l_{i,j}$  such that

$$l_{i,j}(1) = -\frac{\psi_{i,j}(1)}{\mu_i(1) - \mu_i(1)},\tag{C.4}$$

in order for (C.3) to coincide with (C.2b) at x = 1 (see Hu et al. (2016, Rem. 6)). Finally, the segmented kernels are subject to continuity conditions

$$\forall i < p, \forall j \neq p:$$
  $\ell_{i,i}^{p-1}(x, \rho_i^p(x)) = \ell_{i,i}^p(x, \rho_i^p(x)),$  (C.5a)

$$\forall i < p:$$
  $\mathbf{k}_{i}^{p-1}(x, \rho_{i}^{p}(x)) = \mathbf{k}_{i}^{p}(x, \rho_{i}^{p}(x)),$  (C.5b)

for  $1 \le i \le p \le m$  and j = 1, ..., m. It follows by Hu et al. (2019, Thm A.1) that the kernel equations (C.1)–(C.5) have well-posed solutions, which are additionally continuous on every  $\mathcal{T}_i^p$ .

#### References

- Alleaume, V., & Krstic, M. (2025). Ensembles of hyperbolic PDEs: Stabilization by backstepping. *Institute of Electrical and Electronics Engineers. Transactions on Automatic Control*, 70, 905–920.
- Anfinsen, H., & Aamo, O. M. (2019). *Adaptive control of hyperbolic PDEs*. Springer. Auriol, J., & Bresch-Pietri, D. (2022). Robust state-feedback stabilization of an underactuated network of interconnected n+m hyperbolic PDE systems. *Automatica*, 136, Article 110040.
- Auriol, J., & Di Meglio, F. (2016). Minimum time control of heterodirectional linear coupled hyperbolic PDEs. *Automatica*, 71, 300–307.
- Auriol, J., Morris, K. A., & Di Meglio, F. (2019). Late-lumping backstepping control of partial differential equations. Automatica, 100, 247–259.
- Bastin, G., & Coron, J.-M. (2016). Stability and boundary sabilization of 1-d hyperbolic systems. [Cham]: Birkhäuser/Springer.
- Bhan, L., Shi, Y., & Krstic, M. (2024). Neural operators for bypassing gain and control computations in PDE backstepping. *Institute of Electrical and Electronics Engineers. Transactions on Automatic Control*, 69(8), 5310–5325.
- Bikia, V. (2021). Non-invasive monitoring of key hemodynamical and cardiac parameters using physics-based modelling and artificial intelligence [Ph.D. thesis], FPFL
- Burkhardt, M., Yu, H., & Krstic, M. (2021). Stop-and-go suppression in two-class congested traffic. *Automatica*, 123, Article 109381.
- Coron, J.-M., Hu, L., & Olive, G. (2017). Finite-time boundary stabilization of general linear hyperbolic balance laws via Fredholm backstepping transformation. *Automatica*, 84, 95–100.
- Coron, J.-M., Hu, L., Olive, G., & Shang, P. (2021). Boundary stabilization in finite time of one-dimensional linear hyperbolic balance laws with coefficients depending on time and space. *Journal of Differential Equations*, 271, 1109–1170
- Di Meglio, F., Bribiesca Argomedo, F., Hu, L., & Krstic, M. (2018). Stabilization of coupled linear heterodirectional hyperbolic PDE-ODE systems. *Automatica*, 87, 281–289.
- Di Meglio, F., Kaasa, G.-O., Petit, N., & Alstad, V. (2011). Slugging in multiphase flow as a mixed initial-boundary value problem for a quasilinear hyperbolic system. In *American control conference*.
- Di Meglio, F., Vazquez, R., & Krstic, M. (2013). Stabilization of a system of n+1 coupled first-order hyperbolic linear PDEs with a single boundary input. Institute of Electrical and Electronics Engineers. Transactions on Automatic Control, 58, 3097–3111.
- Diagne, A., Diagne, M., Tang, S., & Krstic, M. (2017). Backstepping stabilization of the linearized *Saint-Venant-Exner* model. *Automatica*, 76, 345–354.
- Friedrich, J., Göttlich, S., & Osztfalk, M. (2022). Network models for nonlocal traffic flow. *ESAIM. Mathematical Modelling and Numerical Analysis*, 56(1), 213–235.
- Göttlich, S., Herty, M., Moutari, S., & Weissen, J. (2021). Second-order traffic flow models on networks. SIAM Journal on Applied Mathematics, 81, 258–281.
- Guan, L., Prieur, C., Zhang, L., Prieur, C., Georges, D., & Bellemain, P. (2020). Transport effect of COVID-19 pandemic in France. *Annual Reviews in Control*, 50, 394–408.
- Herty, M., & Klar, A. (2003). Modeling, simulation, and optimization of traffic flow networks. SIAM Journal on Scientific Computing, 25, 1066–1087.
- Hochstadt, H. (1989). Integral equations (Wiley Classics ed.). John Wiley & Sons. Hu, L., Di Meglio, F., Vazquez, R., & Krstic, M. (2016). Control of homodirectional and general heterodirectional linear coupled hyperbolic PDEs. Institute of Electrical and Electronics Engineers. Transactions on Automatic Control, 61, 3301–3314.
- Hu, L., Vazquez, R., Di Meglio, F., & Krstic, M. (2019). Boundary exponential stabilization of 1-dimensional inhomogeneous quasi-linear hyperbolic systems. SIAM Journal on Control and Optimization, 57(2), 963–998.
- Humaloja, J.-P., & Bekiaris-Liberis, N. (2025a). On computation of approximate solutions to large-scale backstepping kernel equations via continuum approximation. *Systems & Control Letters*, 196, Article 105982.
- Humaloja, J.-P., & Bekiaris-Liberis, N. (2025b). Stabilization of a class of large-scale systems of linear hyperbolic PDEs via continuum approximation of exact backstepping kernels. *Institute of Electrical and Electronics Engineers*. *Transactions on Automatic Control*, 70, 5957–5972.

- Iannelli, M. (1995). Mathematical theory of age-structured population dynamics. Giardini Editori e Stampatori in Pisa.
- Kitsos, C., Besancon, G., & Prieur, C. (2022). High-gain observer design for a class of quasi-linear integro-differential hyperbolic systems-application to an epidemic model. *Institute of Electrical and Electronics Engineers. Transactions on Automatic Control*, 67, 292–303.
- Mohan, R., & Ramadurai, G. (2017). Heterogeneous traffic flow modelling using second-order macroscopic continuum model. *Physics Letters*, 381, 115–123.
- Ramirez, H., Zwart, H., & Gorrec, Y. L. (2013). Exponential stability of boundary controlled port Hamiltonian systems with dynamic feedback. In IFAC workshop on control of systems governed by partial differential equation (pp. 115–120).
- Reymond, P., Merenda, F., Perren, F., Rufenacht, D., & Stergiopulos, N. (2009). Validation of a one-dimensional model of the systemic arterial tree. *American Journal of Physiology-Heart and Circulatory Physiology*, 297, H208–H222.
- Tao, T. (2011). An introduction to measure theory. American Mathematical Society. Teschl, G. (2012). Ordinary differential equations and dynamical systems. American Mathematical Society.
- Tucsnak, M., & Weiss, G. (2009). Observation and control for operator semigroups. Birkhäuser Verlag AG.
- Tumash, L., Canudas-de Wit, C., & Delle Monache, M. L. (2022). Multi-directional continuous traffic model for large-scale urban networks. *Transportation Research Part B: Methodological*, 158, 374–402.
- Vazquez, R., Chen, G., Qiao, J., & Krstic, M. (2023). The power series method to compute backstepping kernel gains: theory and practice. In *IEEE conf. decis.* control (pp. 8162–8169).
- Vazquez, R., & Krstic, M. (2008). Control of turbulent and magnetohydrodynamic channel flows. Birkhäuser Boston.
- Yu, H., & Krstic, M. (2021). Output feedback control of two-lane traffic congestion. *Automatica*. 125. Article 109379.
- Yu, H., & Krstic, M. (2022). Traffic congestion control by PDE backstepping. [Cham]: Birkhäuser/Springer.
- Zhang, L., Luan, H., Lu, Y., & Prieur, C. (2022). Boundary feedback stabilization of freeway traffic networks: ISS control and experiments. *IEEE Transactions on Control Systems Technology*, 30, 997–1008.



**Jukka-Pekka Humaloja** received the Ph.D. degree in engineering and natural sciences from Tampere University (of Technology — 2018), Finland, in 2019, where he also was a Postdoctoral Research Fellow from 2019 to 2021. From 2021 to 2023 he was a Postdoctoral Fellow with University of Alberta, Canada, and in 2024, he was a Visiting Lecturer with Aalto University, Finland. Currently he is a Postdoctoral Associate with the Technical University of Crete, Greece. His research interests include control and estimation of distributed parameter systems and large-scale systems, especially robust

output regulation and model predictive control of boundary-controlled PDEs, and virtual decomposition control. He is the recipient of personal postdoctoral grants from the Jenny and Antti Wihuri Foundation (2021–2022) and the Vilho, Yrjö and Kalle Väisälä Foundation (2022–2023).



Nikolaos Bekiaris-Liberis received the Ph.D. degree in aerospace engineering from University of California, San Diego in 2013. From 2013 to 2014, he was a Post-Doctoral Researcher with University of California, Berkeley. From 2019 to 2022, he was an Assistant Professor, from 2017 to 2019, he was a Marie Sklodowska-Curie Fellow, and from 2014 to 2017, he was a Research Associate with the Technical University of Crete, Greece, where he is currently an Associate Professor with the Department of Electrical and Computer Engineering. He has authored/coauthored one

book and more than 140 papers. His research interests include nonlinear delay, switched, and distributed parameter systems, and their applications to transport systems. He serves as Associate Editor for Automatica and as Senior Editor for IEEE Transactions on Intelligent Transportation Systems. He received the Chancellor's Dissertation Medal in Engineering from University of California, San Diego in 2014 and the George N. Saridis Outstanding Research Paper Award in 2019 (from the IEEE Intelligent Transportation Systems Society). He was a recipient of a 2016 Marie Sklodowska-Curie Individual Fellowship Grant and he received a 2022 European Research Council (ERC) Consolidator Grant .